“Influence of polar amino acids in the evolution of the phenylalanine and phenylalanine dipeptide self-assembly: towards the study of diverse morphologies”

M.Sc. Thesis

By

Sheetal Leva

Roll No. 2303131025

Department of Chemistry
Indian Institute of Technology Indore

May 2025

“Influence of polar amino acids in the evolution of the phenylalanine and phenylalanine dipeptide self-assembly: towards the study of diverse morphologies”

A THESIS

Submitted in partial fulfillment of the

requirements for the award of the degree

of

Master of Science

by

Sheetal Leva

Department of Chemistry
Indian Institute of Technology Indore

May 2025

INDIAN INSTITUTE OF TECHNOLOGY INDORE

CANDIDATE'S DECLARATION

I hereby certify that the work being presented in the thesis entitled **"Influence of polar amino acids in the evolution of the phenylalanine and phenylalanine dipeptide self-assembly: towards the study of diverse morphologies"** is the partial fulfilment of requirements for the award of the degree of **MASTER OF SCIENCE** and submitted in the **DEPARTMENT OF CHEMISTRY, Indian institute of technology Indore**, is an authentic record of my work carried out during the time from July 2024 to May 2025 under the supervision of Prof. Anjan Chakraborty, professor, IIT Indore.

I have not submitted the matter presented in this thesis for the award of any other degree of this or any other institute.

Leva

20.05.25

Signature of the student with the date

(Sheetal Leva)

This is to certify that the above statement by the candidate is correct to the best of my knowledge.

AChakraborty

20.05.25

Signature of the Supervisor with the date

(Prof. Anjan Chakraborty)

Acknowledgments

I am deeply grateful to **Prof. Anjan Chakraborty**, my supervisor at IIT Indore’s Chemistry department. His unwavering support and infectious enthusiasm were instrumental in navigating my M.Sc. research journey. Prof. Chakraborty’s dedication to our research group inspired me to strive for excellence. Under his esteemed guidance, I completed my project, and his encouragement motivated me at every step. I am fortunate to have had such a mentor during this pivotal academic endeavour.

I am deeply grateful to **Ms. Priyanka Nath**, my project mentor, for her unwavering guidance and support throughout my research endeavour. Her expertise and encouragement have been invaluable, and I owe a special thanks to her continuous assistance and mentorship, which have significantly contributed to the success of my project.

Thank Dr. Debanjan Bagchi, Mr. Avijit Maity, Ms. Huma Tabassum, Mr. Naveen Kumar, and Mr. Suman Choudhury for their constant support throughout this project.

Moreover, I am filled with gratitude to my family and friends for staying with me in this journey.

Sheetal Leva

2303131025

Dedication

To my beloved parents,

This thesis is lovingly dedicated.

Abstract

Self-assembly is a natural process where disordered molecules organize into structured formations, playing a crucial role in the development of amyloid fibrils associated with degenerative diseases such as Alzheimer's, Parkinson's, and type 2 diabetes. L-phenylalanine (Phe), an essential aromatic amino acid required for protein synthesis, also serves as a precursor for important biomolecules like tyrosine and dopamine. Under certain physiological conditions, excess Phe can aggregate into amyloid fibrils, which contribute to neurotoxic effects observed in metabolic disorders such as phenylketonuria (PKU). However, diphenylalanine (Phe-Phe) peptides, which serve as core recognition motifs of amyloid plaques associated with neurological disorders like Alzheimer's and Parkinson's, are also of particular interest. The formation of these fibrils is driven by interactions like hydrogen bonding, π-π stacking, and van der Waals' forces, leading to structures with hydrophobic surfaces and charged cores that disrupt cellular functions and contribute to toxicity. This research explores the influence of polar amino acids on the self-assembly of L-Phe and Phe-Phe. The results show that polar amino acids, including L-arginine, L-lysine, and L-glutamic acid, effectively inhibit the formation of Phe fibrillar structures. Specifically, L-arginine and L-lysine demonstrate strong capability to prevent fibril development in Phe-Phe systems. Observations were validated using optical microscopy, Confocal laser scanning microscopy, Scanning electron microscopy, UV-visible spectroscopy, and Zeta potential. These findings suggest that polar amino acids can modulate amyloid aggregation, providing valuable insights into potential strategies for managing diseases related to amyloid fibril formation.

Table of contents

List of figures
Acronyms
Abbreviations
Objective
Literature survey
Motivation
Chapter 1: Introduction

1.1 Self-assembly……………………………………………… 1
1.2 Types of self-assembly………………………………… 1
1.2.1 protein and peptide self-assembly…………………… 1
1.2.2 Lipid self-assembly…………………………………… 2
1.2.3 Amino acid self-assembly…………………………….. 2
1.3 L-phenylalanine and Phenylalanine dipeptide self-assembly…………………………………………………... 2-3
1.4 Effect of external factors on self-assembly……………… 3
1.4.1 Effect of concentration……………………………... 3
1.4.2 Effect of pH…………………………………………… 4
1.4.3 Effect of metal ions…………………………………… 4
1.5 Classification of Amino Acids………………………….. 5
1.5.1 Non-polar amino acids………………………………… 5
1.5.2 Polar uncharged amino acids…………………………. 5
1.5.3 Acidic amino acids……………………………………. 6
1.5.4 Basic amino acids…………………………………….. 6

Chapter 2: Experimental section

2.1 Reagents and materials…………………………………. 7
2.2 Instrumentation…………………………………………. 7
2.3 Method……………………………………………………. 8
2.3.1 Preparation of self-assembly of phenylalanine……….. 9
2.3.2 Preparation of self-assembly of phenylalanine dipeptide 9
2.3.3 Preparation of co-assembly of amino acids…………… 9

Chapter 3: Results and discussion

3.1 Self-assembly of phenylalanine…………………………. 9
3.2 Self-assembly of phenylalanine dipeptide………………. 9-10
3.3 Co-assembly of phenylalanine and arginine…………….. 10-13
3.4 Co-assembly of phenylalanine and lysine……………….. 13-16
3.5 Co-assembly of phenylalanine and glutamic acid……….. 16-18
3.6 Co-assembly of phenylalanine and aspartic acid……….. 18-20
3.7 Co-assembly of Phe-Phe and arginine………………….. 20-21
3.8 Co-assembly of Phe-Phe and lysine……………………... 21-22
3.9 Co-assembly of Phe-Phe with glutamic acid and aspartic acid……………………………………………………... 22-23
Future scope 25
Conclusions 25
Supporting information 27-30
References 31-34

List of figures

Figure 01	Biomolecules self-assembly.	xiv
Figure 02	Inhibition of Phe amyloid fibrillar morphology by metal ions.	xvi
Figure 03	Flow chart of the formation of Phe self-assembly.	03
Figure 04	Structures of Nonpolar Amino Acids.	05
Figure 05	Structures of polar amino acids.	06
Figure 06	Structures of acidic amino acids.	06
Figure 07	Structures of basic amino acids	06
Figure 08	(A) Phe structure, time-dependent (B) OM images, (C) CLSM images, (D) Zeta potential of Phe self-assembly.	09
Figure 09	(A) Phe-Phe structure, time-dependent (B) OM images, (C) CLSM images, (D) Zeta potential of Phe-Phe self-assembly.	10
Figure 10	Time-dependent OM images of blank Arg.	11
Figure 11	Time-dependent OM images of the co-assembly of Phe and Arg.	11
Figure 12	Time-dependent CLSM images of co-assembly of Phe and Arg (1:2 ratio).	12
Figure 13	(A) Time-dependent SEM images of co-assembly of Phe and Arg (1:2 ratio), (B) UV-visible spectra of blank Phe, blank Arg, and co-assembly of Phe and Arg, (C) Time-dependent Zeta potential of co-assembly of Phe and Arg.	13
Figure 14	Time-dependent OM images of blank Lys.	14
Figure 15	Time-dependent OM images of the co-assembly of Phe and Lys.	14
Figure 16	Time-dependent CLSM images of co-assembly of Phe and Lys (1:2 ratio).	15
Figure 17	(A) Time-dependent SEM images of co-assembly of Phe and Lys (1:2 ratio), (B) UV-visible spectra of blank Phe, blank Lys, and co-assembly of Phe and Lys, (C) Time-dependent Zeta potential of co-assembly of Phe and Lys.	16
Figure 18	Time-dependent OM images of blank Glu.	16
Figure 19	Time-dependent OM images of co-assembly of Phe and Glu (1:2 ratio).	17
Figure 20	CLSM images of the co-assembly of Phe and Glu (1:2 ratio).	17
Figure 21	(A) Time-dependent SEM images of co-assembly of Phe and Glu (1:2 ratio), (B) UV-visible spectra of blank Phe, blank Glu, and co-assembly of Phe and Glu, (C) Time-dependent Zeta potential of co-assembly of Phe and Glu.	18
Figure 22	Time-dependent OM images of blank Asp.	18

Figure 23 Time-dependent OM images of the co-assembly of Phe and Asp. 19
Figure 24 Time-dependent CLSM images of co-assembly of Phe and Asp (1:2 ratio). 19
Figure 25 A) Time-dependent SEM images of co-assembly of Phe and Asp (1:2 ratio), (B) UV-visible spectra of blank Phe, blank Asp, and co-assembly of Phe and Asp, (C) Time-dependent Zeta potential of co-assembly of Phe and Asp. 20
Figure 26 Time-dependent CLSM images of co-assembly of Phe-Phe and Arg (1:2 ratio). 21
Figure 27 (A) Time-dependent SEM images of co-assembly of Phe-Phe and Arg (1:2 ratio), (B) UV-visible spectra of blank Phe-Phe, blank Arg, and co-assembly of Phe-Phe and Arg, (C) Time-dependent Zeta potential of co-assembly of Phe-Phe and Arg. 21
Figure 28 Time-dependent CLSM images of co-assembly of Phe-Phe and Lys (1:2 ratio). 22
Figure 29 A) Time-dependent SEM images of co-assembly of Phe-Phe and lysine (1:2 ratio), (B) UV-visible spectra of blank Phe-Phe, blank Lys, and co-assembly of Phe and Lys, (C) Time-dependent Zeta potential of co-assembly of Phe-Phe and Lys. 22
Figure 30 Images of (A) Co-assembly of Phe-Phe and Glu, (B) Co-assembly of Phe-Phe and Asp, (C) Self-assembly of Phe-Phe. 23
Figure 31 (A)Time-dependent CLSM images of the co-assembly of Phe-Phe and Glu. (B) Time-dependent Zeta potential of co-assembly of Phe-Phe and Glu. 23
Figure 32 (A)Time-dependent CLSM images of the co-assembly of Phe-Phe and Asp. (B) Time-dependent Zeta potential of the co-assembly of Phe-Phe and Asp. 23

Acronyms

Arg	Arginine
Asp	Aspartic acid
Asn	Asparagine
CLSM	Confocal laser scanning microscope
Glu	Glutamic acid
Gln	Glutamine
His	Histidine
Lys	Lysine
Phe	Phenylalanine
Phe-Phe	Phenylalanine dipeptide
OM	Optical microscope
Ser	Serine
SEM	Scanning electron microscope
Thr	Threonine
ThT	Thioflavin T

Abbreviation

mg	Milligram
mol	Mole
g	Gram
mL	Milliliter
°C	Degree Celsius
%	Percentage
h	Hour
min	Minutes
μM	Micro molar
μm	Micrometer

Objective

To understand the object of this research, it's essential to know the self-assembly of biomolecules, such as phenylalanine and its dipeptide. Phenylalanine and diphenylalanine form amyloid fibrillar structures under normal physiological conditions, which are the main motif of many degenerative diseases. This research aims to investigate how various biomolecules influence the amyloid fibrillar structures formed by phenylalanine and diphenylalanine during self-assembly under physiological conditions. So, here we specifically focus on understanding how polar amino acids, naturally present in the body, influence the amyloid fibrillar structure. The primary aim of this work is to understand how polar amino acids influence the formation of amyloid aggregates.

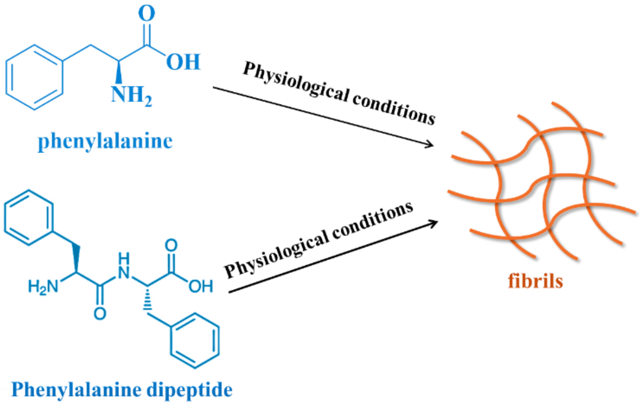

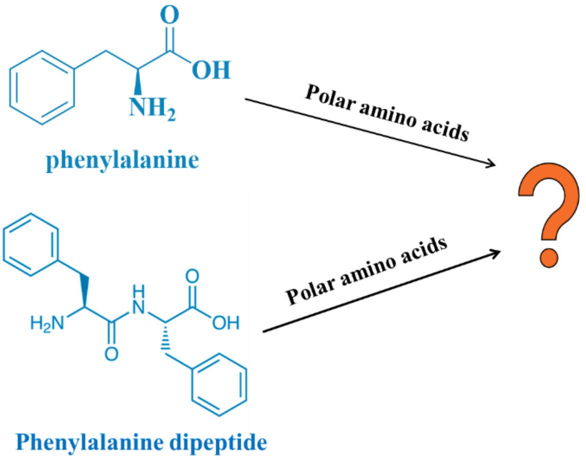

Literature survey

Self-assembly is the process in which molecules spontaneously and selectively organize themselves into well-structured formations, driven by noncovalent interactions such as electrostatic interactions, van der Waals' forces, π-π stacking interactions, and hydrogen bonding.[1],[2] Biomolecules like proteins, peptides, nucleotides, and amino acids are well known for forming self-assembly.[3] Research has demonstrated that proteins and peptides can form nanostructures, including nanowires, nanofibers, nanospheres, nanovesicles, nanogels, nanobelts, and nanotubes.[4] Self-assembly not only enhances the mechanical stability and strength of these molecules but also amplifies their natural activity through the collective behavior of the assembled structures.[5] This process plays a crucial role in numerous cellular functions. However, when aggregation becomes uncontrolled, it can result in the development of amyloid fibrils, which cause several illnesses, including Alzheimer's, type II diabetes, and Parkinson's disease (6).

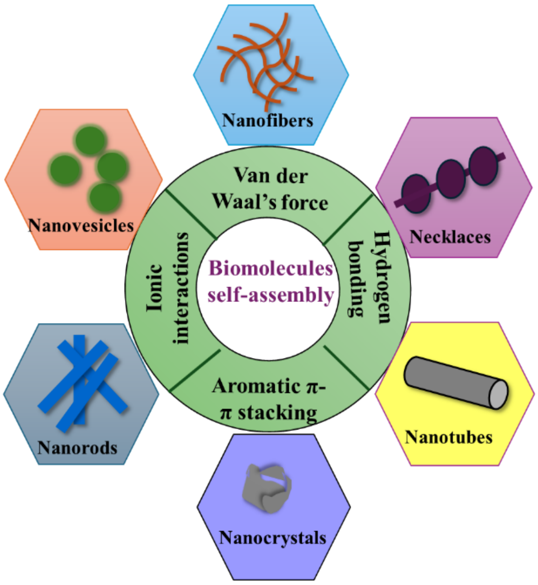

Figure 01: Biomolecules self-assembly.

Amino acids, the fundamental building blocks of peptides and proteins, possess the ability to undergo self-assembly.[7] Among various amino acids, phenylalanine and its dipeptide are particularly notable for their ability to form fibrillar structures resembling amyloids, which also display cytotoxic properties. The self-assembly of phenylalanine is particularly important in the context of phenylketonuria (PKU), a metabolic disorder.[8] However, diphenylalanine self-assembly is associated with neurological disorders like Parkinson's and Alzheimer's. Adler Abramovich and colleagues show that Phe, an aromatic amino acid, forms an ordered nanoscale fibrillar structure. [9] These aggregates display properties similar to amyloid fibrils, suggesting a potential for developing amyloid-related diseases. [10]

Several studies have indicated that factors such as pH, protein or peptide concentration, and the presence of ions can greatly influence the process of amyloid aggregation.[11],[12] The Sarkar group explored that crown ethers (CEs) can disrupt Phe amyloid fibril formation. (13) The Gazit Group reported that polyphenols such as Epigallocatechin gallate (EGCG) and Tannic acid (TA) inhibit the formation of Phe fibrils. (14) The Panda group demonstrated that L-Dopa-functionalised gold nano-roses (GNRs) effectively disaggregate amyloid-like fibrils formed by the Phe-Phe. (15) Co-assembly with amino acids may prevent the development of fibril structure based on Phe, according to several recent findings. D-phenylalanine (D-Phe) has been shown by Thakur and associates to prevent L-Phe from forming fibrils. (16) Furthermore, the effect of co-assembly with several aliphatic chain amino acids (ACAAs), including alanine (Ala), leucine (Leu), isoleucine (Ile), and valine (Val), on the suppression of Phe-based fibrils was examined by Shamra and Wangoo's group. (17)

Motivation

Our lab previously reported the impact of metal ions on the self-assembled structures of Phe. We used metal ions of varying charge and size ratios to examine their effects. Our findings revealed that monovalent ions (such as Na^{+}) and divalent ions (such as Mg^{2+} and Ca^{2+}, except Zn^{2+}, $Cd^{2+,}$ and Hg^{2+}) did not significantly alter the emission patterns or morphology of the structures formed by Phe. In contrast, trivalent metal ions, including Al^{3+}, Ga^{3+}, and In^{3+}, inhibited the formation of long fibrillar structures by promoting nano-aggregate development.

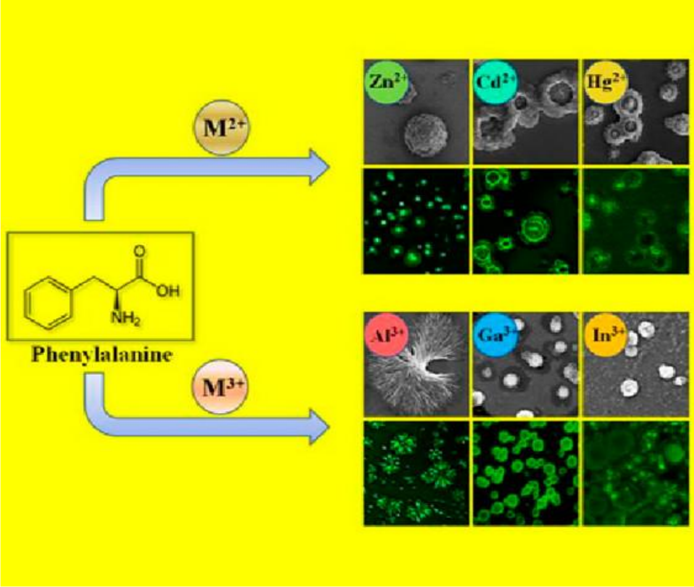

Figure 02: Inhibition of Phe amyloid fibrillar morphology by metal ions.

So here we are, interested in investigating the factors that influence the formation of Phe and its dipeptide self-assembly into amyloid fibrils under physiological conditions. Specifically, we are studying how polar amino acids interact with Phe and Phe-Phe, and how they affect its self-assembly process.

Chapter 1: Introduction

1.1 Self-assembly

Molecular self-assembly is a highly effective strategy for constructing novel supramolecular architectures and is a phenomenon extensively observed in biological systems, where it plays a fundamental role in various natural processes. This self-directed organization arises from weak, noncovalent interactions including hydrogen bonding, ionic (electrostatic) forces, hydrophobic interactions, van der Waals' forces, and water-mediated hydrogen bonds which, although individually weak, collectively dictate the structural conformation of biological macromolecules and regulate their interactions with other molecular species. Among these macromolecules, proteins, peptides, nucleotides, and amino acids are well known for their intrinsic ability to undergo self-assembly, giving rise to diverse nanostructures such as nanowires, nanofibers, nanospheres, nanovesicles, nanogels, nanobelts, and nanotubes.[19] These well-organized architectures exhibit not only enhanced mechanical stability but also functional properties arising from the cooperative behaviour of their constituent molecules, contributing to a wide range of essential cellular activities. Biomolecular self-assembly plays a pivotal role in numerous biological processes, including cell membrane formation, enzyme activity, and structural protein folding. However, while self-assembly is crucial for biological organization and functionality, its dysregulation can lead to pathological outcomes. In particular, uncontrolled aggregation of self-assembling biomolecules such as proteins, peptides, and amino acids can lead to the formation of amyloid fibrils, highly ordered β-sheet-rich structures linked to various protein misfolding diseases, including Alzheimer's disease, Parkinson's disease, and type II diabetes.[20][21] Additionally, many human degenerative disorders are associated with the formation of organized amyloid fibrils from proteins, polypeptides, and dipeptides. Therefore, gaining a clear understanding of their fundamental self-assembly mechanisms is essential. Exploring the different types of self-assembly is also important to enhance this understanding.

1.2 Types of Biomolecular Self-Assembly

1.2.1 Peptide and Protein Self-Assembly:

Peptides and proteins exhibit a remarkable capacity to spontaneously organize into various supramolecular architectures, including nanofibrils, nanotubes, two-dimensional sheets, and hydrogel networks.[22] One of the most thoroughly investigated assemblies is the amyloid fibril, typically characterized by the cross-β motif formed via beta-sheet stacking.[23]

1.2.2 Lipid Self-Assembly:

Lipids spontaneously form micelles, bilayers, and vesicles in aqueous environments driven by the hydrophobic effect. These structures are essential to cellular membrane formation and serve as model systems in synthetic biology and drug delivery.

1.2.3 Amino Acid Self-Assembly:

Single amino acids, especially aromatic ones like phenylalanine, tyrosine, and tryptophan, can self-assemble into a variety of nanostructures such as fibrils, nanotubes, and crystals. These assemblies are primarily driven by π-π stacking interactions, hydrogen bonding, and hydrophobic effects. Adler Abramovich and colleagues show that Phe, an aromatic amino acid, forms an ordered nanoscale fibrillar structure. And the Phe-Phe, which serve as core recognition motifs of amyloid plaques associated with neurological disorders like Alzheimer's and Parkinson's, are of particular interest. Biological molecules, including proteins, peptides, dipeptides, and amino acids, are involved in the self-assembly. However, due to the structural complexity of proteins and peptides, the underlying mechanisms behind the self-assembly process remain elusive. Therefore, single amino acids and small dipeptides have garnered attention in recent years.

1.3 L-phenylalanine and phenylalanine dipeptide self-assembly

L-phenylalanine (Phe) is an essential amino acid that is crucial for protein synthesis and various metabolic functions. It is crucial for the growth and development of the human body. Additionally, Phe serves as a precursor for other essential compounds, including tyrosine, dopamine (a neurotransmitter), and melanin. Since our bodies cannot produce Phe on their own, it must be obtained through food or supplements. Phe is naturally present in various plant- and animal-based food sources. Common foods rich in this amino acid include breast milk, meat, fish, eggs, nuts, seeds, and soya products.

However, under certain physiological conditions, Phe can self-assemble into amyloid fibrillar, which are organized protein aggregates linked to diseases such as Alzheimer's disease, Parkinson's disease, and type 2 diabetes. And also The Phe-Phe dipeptide, a key motif in amyloid fibrils, self-assembles through π-π stacking interactions, hydrogen bonding, and hydrophobic effects, leading to ordered supramolecular architectures This formation of amyloid fibrillar is particularly significant in the case of Phenylketonuria (PKU) is a metabolic disorder that results from a deficiency in the enzyme phenylalanine hydroxylase, [24]which leads to an accumulation of phenylalanine. Excess Phe can result in the development of amyloid-like fibrils, contributing to the neurotoxic effects and neurological symptoms observed in PKU patients.

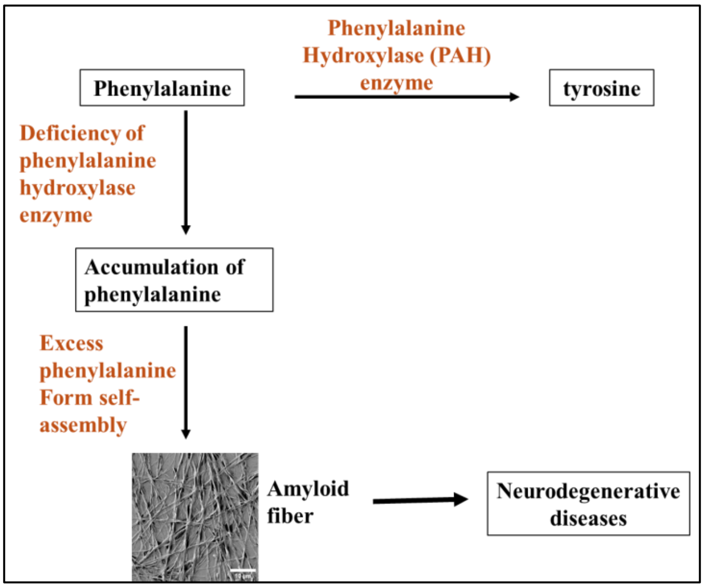

Figure 03: Flow chart of the formation of Phe self-assembly.

Phe and Phe-Phe molecules assemble through interactions such as hydrogen bonding, van der Waals' forces, electrostatic interactions, and π-π stacking. These interactions create a multi-core structure with a hydrophilic core surrounded by a hydrophobic outer surface. The hydrophobic surface allows the fibrils to penetrate cell membranes. During this process, the hydrophilic core, containing charged zwitterionic ends, can cause ion imbalance and lead to cell damage. The hydrophobic outer layer is a key factor in the toxicity of the fibrils. Several studies have shown that Phe and Phe-Phe can form various structures such as nanotubes, nanowires, nanovesicles, and nanofibers during self-assembly. This has sparked significant research into understanding how this process occurs. In this context, many studies indicate that factors such as molecule concentration, pH, and the presence of ions or nanoparticles significantly affect the self-assembly process.

1.4 Effect of External Factors on Self-assembly:

1.4.1 Effect of concentration:

Studies reveal that the concentration of biomolecules significantly influences self-assembly behavior. Shen et al. [25] demonstrated that fibril formation of the β-amyloid protein is highly concentration-dependent. When the concentration was increased to 0.5 g/L or higher, fibrillation occurred rapidly. Also, Phe aggregation typically initiates above a critical aggregation concentration (CAC) in the range of 2–50 mM under physiological conditions. At lower concentrations, Phe exists as monomers or small oligomers, while higher concentrations promote π–π stacking and hydrophobic interactions, leading to well-ordered nanostructures like fibrils and nanotubes. [26]

1.4.2 Effect of pH:

The presence of ionic groups in biomolecules makes the hydrogen ion concentration (pH) of the solution a critical factor in their self-assembly behavior. In general, a reduction in pH tends to favour the formation of amyloid fibrils in proteins. For short peptides, their self-association is largely influenced by the isoelectric point and the pKa values of their constituent amino acids.[27]

1.4.3 Effect of metal ions:

Metal ions are vital to numerous biological functions, including cellular homeostasis and enzymatic activity, through their coordination with key biomolecules. Beyond these roles, recent studies have highlighted their influence on amyloid aggregation. In this aspect, Lovell et.al introduced that high levels of metal ions (such as Zn^{2+}, Cu^{2+}, and Fe^{3+}) are deposited in senile plaques. Additionally, Al^{3+} has been detected in amyloid fibres at the centre of these plaques. [28] However, zinc (Zn^{2+}) seems to stabilize smaller, non-fibrillar amyloid clusters. Studies by Ha and colleagues show that both Zn^{2+} and Cu^{2+} can interfere with the formation of fibrillar amyloid, instead promoting the creation of amorphous, non-fibrillar aggregates. [29] More recently, Ye et al. explored how protein nanofibrils (PNFs) grow and form hydrogels in the presence of different metal ions.[30] Overall, these findings suggest that metal ions may play a role in triggering or encouraging the aggregation of proteins or peptides.

However, our previous study showed that divalent ions (Mg^{2+}, Ca^{2+}) had little effect on Phe self-assembly. In contrast, trivalent ions (Al^{3+}, Ga^{3+}, In^{3+}) inhibited fibril formation and caused nano-aggregation, while divalent ions like Zn^{2+}, Cd^{2+}, and Hg^{2+} also disrupted the process.[31] In our lab, we are investigating the interactions between Phe and Phe-Phe with polar amino acids that possess positive and negative charges (such as L-arginine (Arg), L-histidine (His), L-lysine (Lys), L-glutamic acid (Glu), L-aspartic acid (Asp), L-glutamine (Gln), L-asparagine (Asn), L-serine (Ser), and L-threonine (Thr). We are investigating how these interactions affect the morphology of the resulting fibrillar structures during the self-assembly process. This research finds the potential role of polar amino acids in modulating the structure and aggregation of amyloid fibrils.

1.5 Classification of Amino Acids:

Amino acids are organic compounds that feature both a carboxylic acid group (-COOH) and an amino group (-NH_2), along with a distinct organic R group (side chain) for each amino acid. They serve as the building blocks of proteins and are essential for many biological functions, including enzyme activity, cell signaling, and synthesizing neurotransmitters and hormones.

All amino acids, except for glycine, are chiral molecules and exist in two enantiomeric forms: D and L. However, the amino acids found in proteins almost exclusively possess the L configuration. Amino acids are classified into four categories: polar uncharged amino acids, nonpolar amino acids, acidic amino acids, and basic amino acids.

1.5.1 Nonpolar amino acids

Amino acids such as glycine (Gly), alanine (Ala), valine (Val), leucine (Leu), isoleucine (Ile), proline (Pro), phenylalanine (Phe), methionine (Meth), and tryptophan (Trp) are classified as nonpolar amino acids. The R groups of these amino acids contain either aromatic or aliphatic groups, which contribute to their hydrophobic nature.

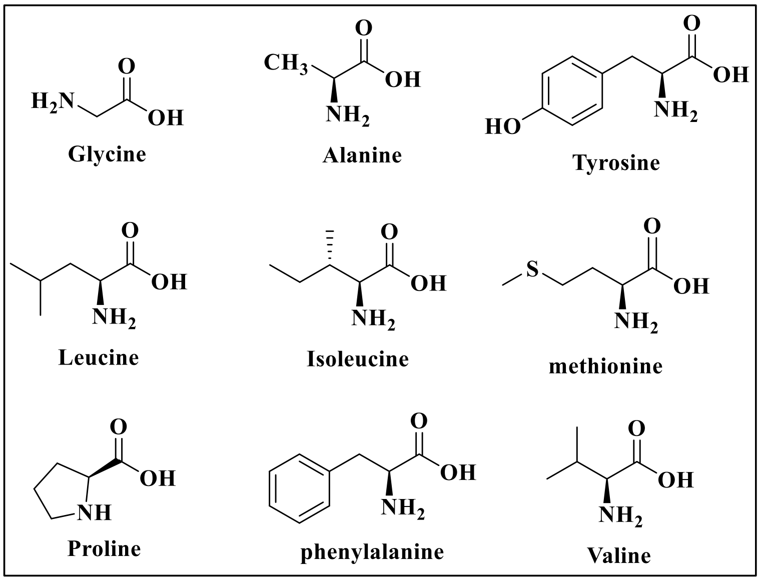

Figure 04: Structures of Nonpolar amino acids.

1.5.2. Polar uncharged amino acids:

Amino acids are serine (Ser), cysteine (Cys), threonine (Thr), tyrosine (Tyr), asparagine (Asn), and glutamine (Gln). The R group of these amino acids is the polar group, which contains electronegative atoms like oxygen, nitrogen, and sulphur. These amino acids are hydrophilic due to this polar group.

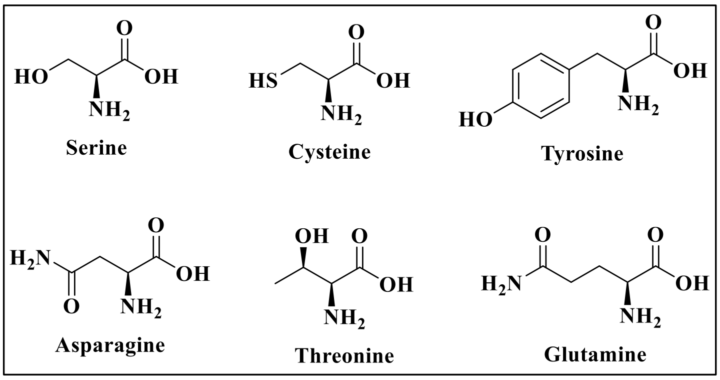

Figure 05: Structures of polar amino acids.

1.5.3. Acidic amino acids:

These amino acids have a carboxylic acid group (-COOH) present in its side chain, and due to this carboxylic acid group, these amino acids are acidic. Asp and Glu are examples of acidic amino acids. The side chain of these amino acids forms ionic bonds.

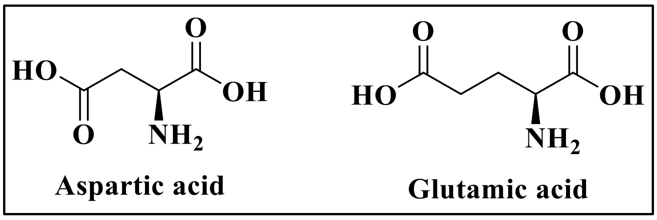

Figure 06: Structures of acidic amino acids.

1.5.4. Basic amino acids

Amino acids Arg, Lys, and His have an amino group ($-NH_2$) in their side chain and due to this group, these amino acids are basic. The side chain of these amino acids forms ionic bonds.

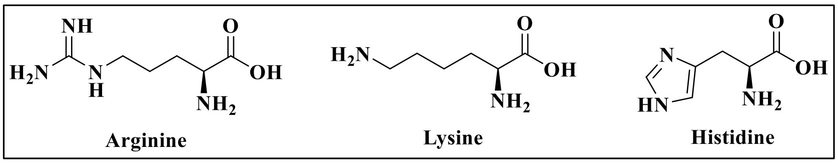

Figure 07: Structures of basic amino acids.

Chapter 2: Experimental Section

2.1 Reagents and materials

Amino acids, namely, L-phenylalanine, L-arginine, L-histidine, L-lysine, L-glutamic Acid, L-aspartic acid, L-glutamine, L-asparagine, L-serine, L-threonine, and 4-(2-hydroxyethyl)-1-piperazineethanesulfonic acid (HEPES), were purchased from SRL. Diphenylalanine, thioflavin T (ThT), and Nile red were purchased from Sigma-Aldrich. Every chemical is used as received, without any additional purification.

2.2 Instrumentation

2.2.1 Optical Microscope

We used a DEWINTER optical microscope for imaging the samples. The optical images of the self-assembled structures of amino acids were captured at a 40X resolution using an in-built camera.

2.2.2. Confocal Laser Scanning Microscopy (CLSM)

We used an OLYMPUS confocal microscope, model IX-83, to image the samples confocally. The Multiline Ar lasers (gas laser) with an excitation wavelength of 488 nm and 559 nm were used to monitor ThT and Nile red-stained aromatic amino acid self-assemblies, respectively. ThT and Nile red concentrations were maintained at 5 µM and 1 µM for all the samples. To extract the solvent, a freshly made sample was drop-cast on a clean glass slide and put in a vacuum desiccator. Every imaging study was conducted at ambient temperature.

2.2.3. Scanning Electron Microscopy (SEM)

A scanning electron microscope, model JEOL-7610 F Plus, was used for SEM imaging. After being vacuum-dried on glass slides, the freshly made samples were covered with gold for SEM investigation at an operating voltage of 5 kV.

2.2.4. Zeta Potential Measurements

The zeta potential of the Phe and Phe-Phe and all co-assembly was measured using a Nano Plus particle size analyser (NanoPlus-3 model). An aliquot of the sample was injected into the capillary chamber, and the zeta potential was measured. Each sample was measured three times for better reproducibility of the result.

2.2.5. UV-Visible Spectroscopy:

We used a Varian UV−vis spectrophotometer (Cary 100 Bio) to record all the UV−vis absorption spectra. Origin Pro 8.1 software was used to analyse all of the absorption spectra.

2.3 Methods

2.3.1 Preparation of Self-Assembly of L-Phenylalanine

Aromatic amino acid Phe (10 mM) was dissolved in HEPES buffer (10 mM, pH ~7.4) and heated at 90°C for 2 hours to achieve the monomeric state. The solution was then gradually cooled to room temperature without any disturbance, resulting in the formation of a fibrillar structure.

2.3.2 Preparation of self-assembly of phenylalanine dipeptide

Phe-Phe (5 mM) was dissolved in HEPES buffer (10 mM, pH ~7.4) and heated at 90°C for 2 hours to achieve the monomeric state. The solution was then gradually cooled to room temperature without any disturbance, resulting in the formation of a fibrillar structure.

2.3.3 Preparation of co-assembly of amino acids

In case of co-assembly, different polar amino acids (such as Arg, His, Lys, Glu, Asp, Gln, Asn, Ser, and Thr) were added to the preheated solution at a 1:2 ratio of Phe or Phe-Phe and amino acids, respectively, before incubating at room temperature.

Chapter 3: Results and discussion

3.1 Phenylalanine self-assembly:

Initially, we investigate the self-assembly of Phe (Figure 8A). To observe the morphology of Phe self-assembly in a time-dependent manner, we first used an optical microscope (OM), which confirmed the formation of a fibril-like structure of the self-assembly (Figure 8B). Subsequently, we confirmed fibrillar morphology using CLSM microscopy (Figure 8C) and zeta potential of Phe self-assembly is negative (-37) at an initial stage. It remains negative till 24 hours, which indicates the fibrillar structure stability. (Figure 8D).

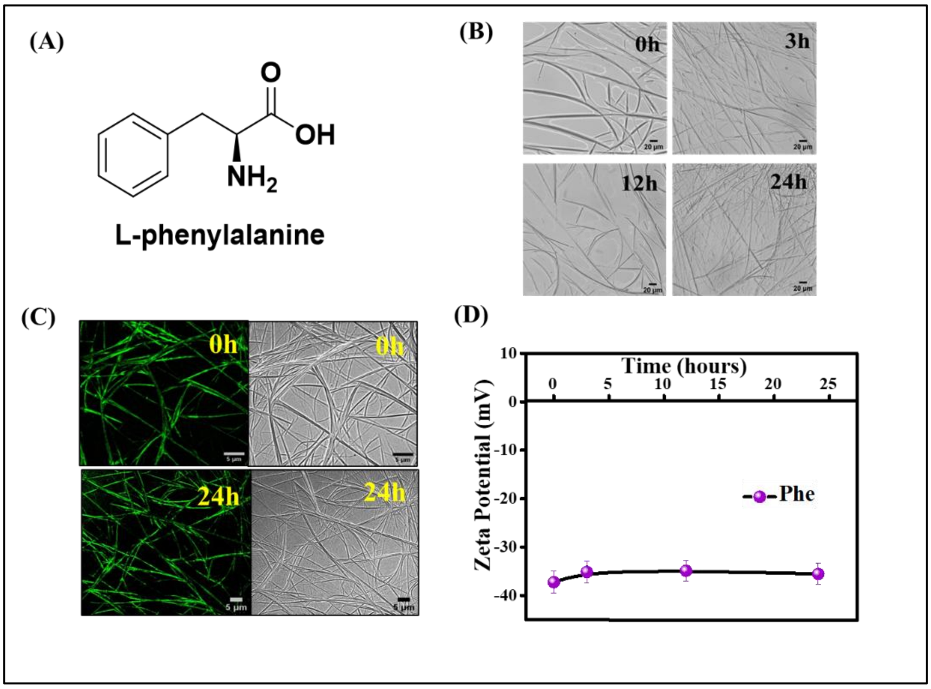

Figure 08: (A) Phe structure**,** time-dependent **(B)** OM images, **(C)** CLSM images, **(D)** Zeta potential of Phe self-assembly.

3.2 Phenylalanine Dipeptide self-assembly:

We investigate the self-assembly of Phe-Phe (Figure 9A). To observe the morphology of Phe-Phe self-assembly in a time-dependent manner, we first used an OM, which confirmed the formation of a fibril-like structure of the self-assembly (Figure 9B). Subsequently, we confirmed fibrillar morphology using CLSM microscopy (Figure 9C) and the Zeta potential of Phe-Phe self-assembly is negative (-28.1) at an initial stage and after 24 hours remains negative, which indicates that the fibrillar structure stability. (Figure 9D).

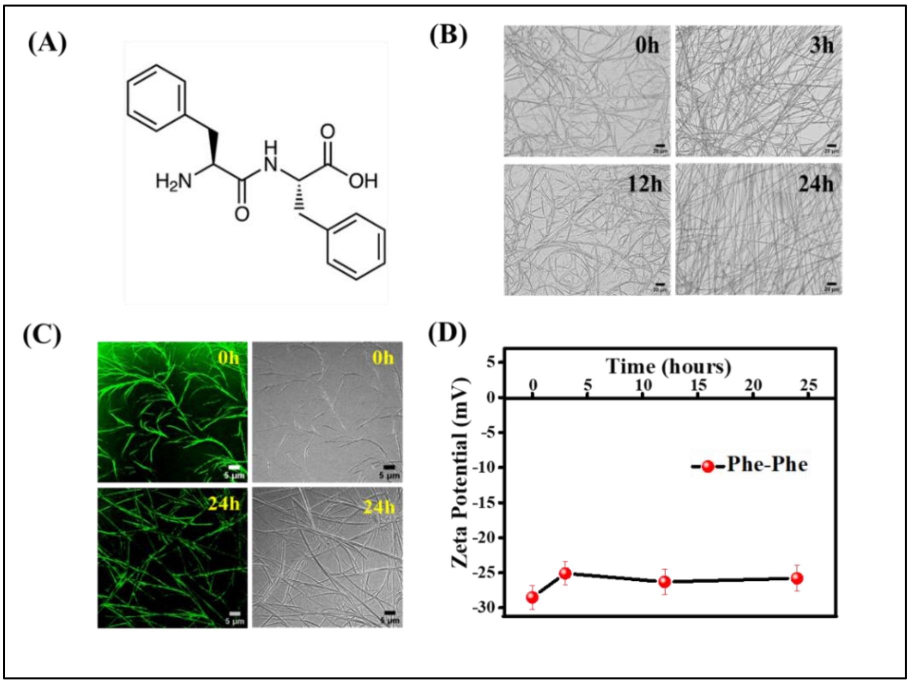

Figure 09: (A) Phe-Phe structure**,** time-dependent **(B)** OM images, **(C)** CLSM images, **(D)** Zeta potential of Phe-Phe self-assembly.

From the above data, it was clear that without external stimuli, Phe and Phe-Phe show no intermediates in the formation of a fibrillar-like structure. Previously, we investigated the effect of different metal ions on the self-assembly of Phe. Here in this work, we explore the impact of polar amino acids on the Phe and its dipeptide self-assembly. For that, we use polar amino acids (such as Arg, His, Lys, Glu, Asp, Gln, Asn, Ser, and Thr). Here, we observe that specific polar amino acids such as Arg, Lys, and Glu successfully inhibit the fibrillar formation of Phe and Phe-Phe. As we want to do a comparative study that is why we further work with four polar amino acids that are two basic amino acids (Arg and Lys) and two acidic amino acids (Glu and Asp).

3.3 Co-assembly of phenylalanine and arginine:

Initially, we studied the interaction between Phe and Arg in a time-dependent manner. From OM images of (Figure 10) observed that blank Arg does not form any prominent morphology. And in OM images (Figure 11), we observed that in a 1:1 ratio, fibrillar morphology was present for 3 hours, but after that, we can see that there is a nanoaggregates-like morphology present with the fibrillar-like morphology. But in case of a 1:2 ratio, an aggregate-like structure resembling a flower-like morphology was observed for 24 hours, and no fibrillar morphology was detected during the same period. In the 1:3 ratio, a large flower-like morphology was observed, which also appeared in the 1:4 ratio observed may be due to the larger content of Arg. For further characterization, we used a 1:2 ratio of Phe to Arg, as this ratio yields the most prominent intermediate structures. We confirmed the morphology for a 1:2 ratio by using time-dependent CLSM analysis (Figure 12). We used ThT, a well-known fluorescence marker for self-assembled fibrillar structures, and Nile red, a fluorescence marker for hydrophobic structures, to tag the co-assembly. Time-dependent SEM analysis confirms the flower-like morphology of the co-assembly (Figure 13A).

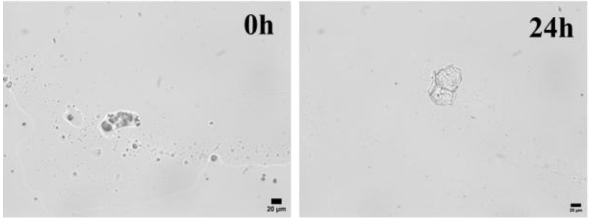

Figure 10: Time-dependent OM images of blank Arg. Scale bar – 20 µm.

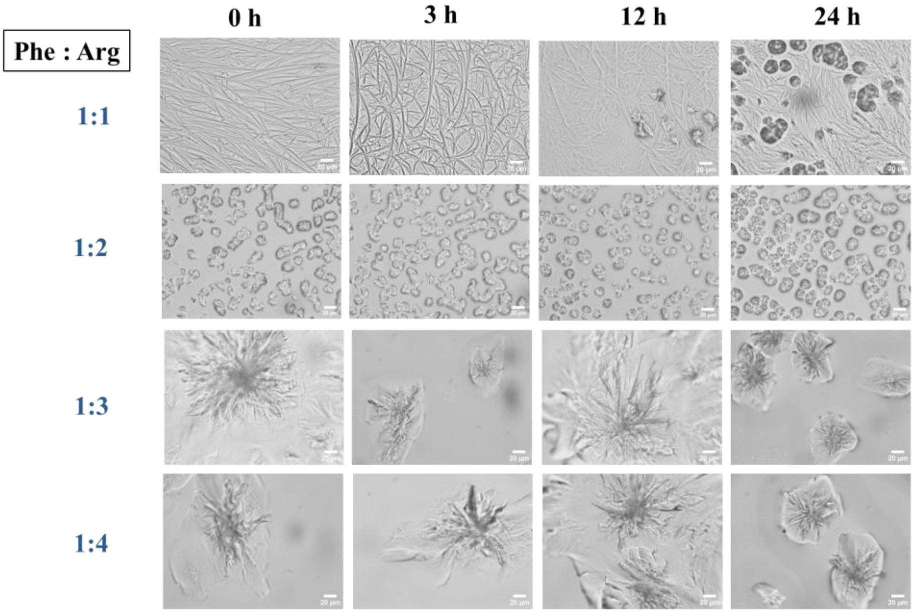

Figure 11: Time-dependent OM images of co-assembly of Phe and Arg. Scale bar - 20µm.

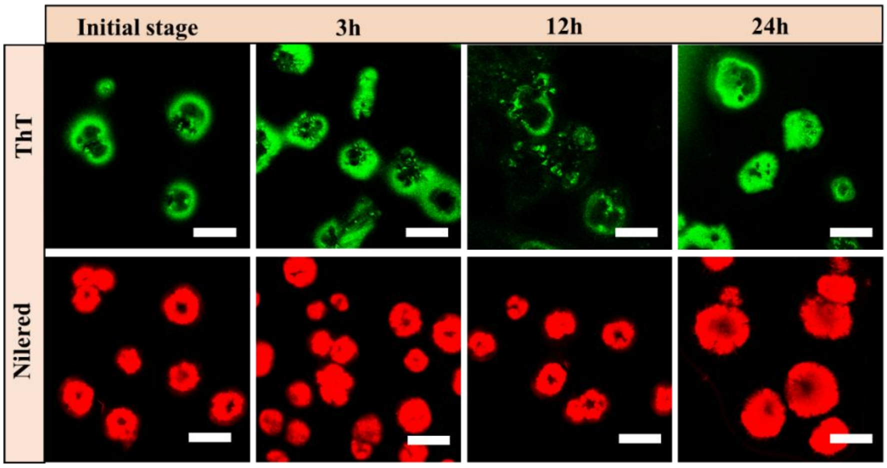

Figure 12: Time-dependent CLSM images of co-assembly of Phe and Arg (1:2 ratio). Scale bar -20 μm.

To further study the effect of polar amino acids interactions on the self-assembly of Phe, we performed UV-vis and Zeta potential. The UV-vis spectra (Figure 13B) of the co-assembly of Phe and Arg presented the combined effect of Phe and Arg, suggesting the absorbance peak at around 258 nm, The intensity of co-assembly increased compared to blank Phe, which indicates that structural changes are occurring, and these changes may be due to the π−π stacking interactions between Phe and Arg. From (Figure 13C) it was observed that Phe shows a negative zeta potential at the initial stage, approximately (-37), and Arg is a positively charged amino acid, and we get a negative zeta potential value for co-assembly, at the initial stage (-34.04), and along with time zeta potential value changed, and we observed (-25.91) after 24 hours. This observation indicates that the negative charge of the Phe self-assembly outer surface may interact with a positive charge of Arg, and these interactions could be a reason for the flower-like morphology formed in place of fibrillar morphology formation. And the zeta potential of co-assembly remains negative till 24 hours, which indicates structural stability.

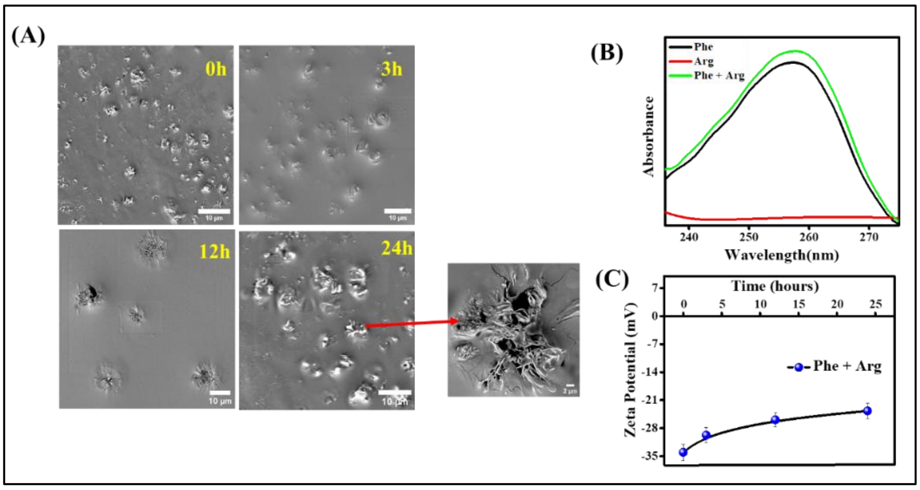

Figure 13: (A) Time-dependent SEM images of co-assembly of Phe and Arg (1:2 ratio), (B) UV-visible spectra of blank Phe, blank Arg, and co-assembly of Phe and Arg, (C) Time-dependent Zeta potential of co-assembly of Phe and Arg.

3.4 Co-assembly of phenylalanine and lysine:

Here, we studied the interaction of Phe with Lys in a time-dependent manner. In OM images (Figure 14), it was observed that blank lysine forms flat vesicle-like morphology. OM images (Figure 15) observed that at a 1:1 ratio, fibrillar morphology was observed at the very initial stage and till 24 hours, which shows that lysine does not inhibit the fibrillar formation. At a 1:2 ratio, an aggregate structure resembling a flower-like morphology was observed at the initial stage, and after 3 hours, aggregates started to fuse, and by 24 hours, aggregates converted into a large aggregate, and there is no fibrillar morphology was detected till 24 hours. In the 1:3 and 1:4 ratio, a large flower-like morphology was observed may be due to the larger content of Lys. For further characterization, we used a 1:2 ratio of Phe to Lys, as this ratio yields the most prominent intermediate structures. We confirmed these results for a 1:2 ratio with CLSM (Figure 16). We used ThT, a well-known fluorescence marker for self-assembled fibrillar structures, and Nile red, a fluorescence marker for hydrophobic structures, to tag the co-assembly, and Time-dependent SEM analysis confirms the flower-like morphology of the co-assembly (Figure 17A).

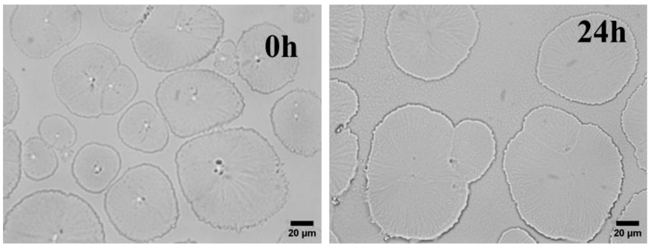

Figure 14: Time-dependent OM images of blank Lys. Scale bar – 20 µm.

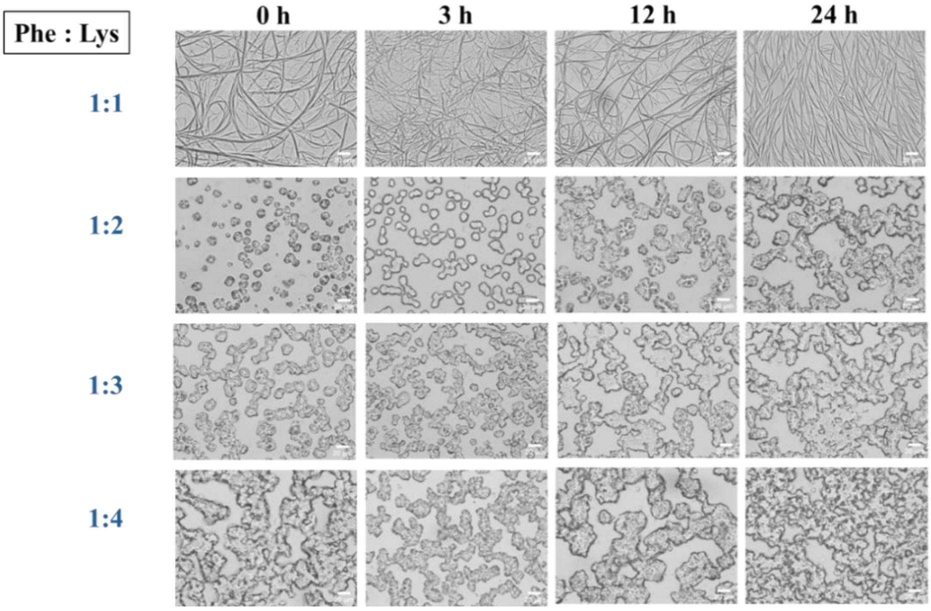

Figure 15: Time-dependent OM images of co-assembly of Phe and Lys. Scale bar – 20 µm.

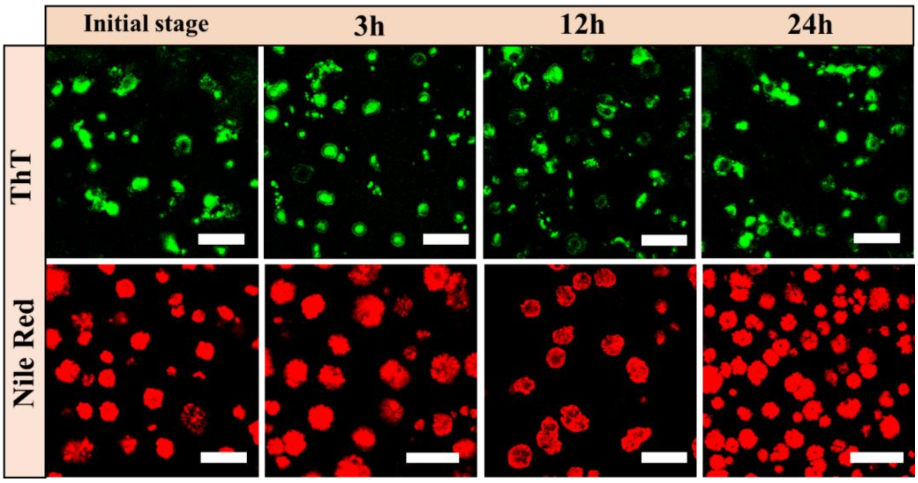

Figure 16: Time-dependent CLSM images of co-assembly of Phe and Lys (1:2 ratio). Scale bar – 20 μm.

To further study the effect of Lys interactions on the self-assembly of Phe, we performed UV-vis and Zeta potential. The UV-vis spectra (Figure 17B) of the co-assembly of Phe + Lys presented the combined effect of Phe and Lys, suggesting that the absorbance peak around 258 nm, Intensity of the co-assembly increased compared to blank Phe, which indicates that structural changes are occurring, and these changes may be due to the π–π stacking interactions between Phe and Lys. Phe shows a negative zeta potential at the initial stage, approx. (-37), and Lys is a positively charged amino acid, and we get a negative zeta potential value for co-assembly (Figure 17C), at the initial stage (-42.79), and along with time zeta potential value increased, and we observed (-31.63) after 24 hours. This observation indicates that the outer surface negative charge of the Phe self-assembly may interact with a positive charge of Lys, and these interactions could be a reason for the flower-like morphology formed in place of fibrillar morphology formation. And the zeta potential of co-assembly remains negative till 24 hours, which indicates structural stability.

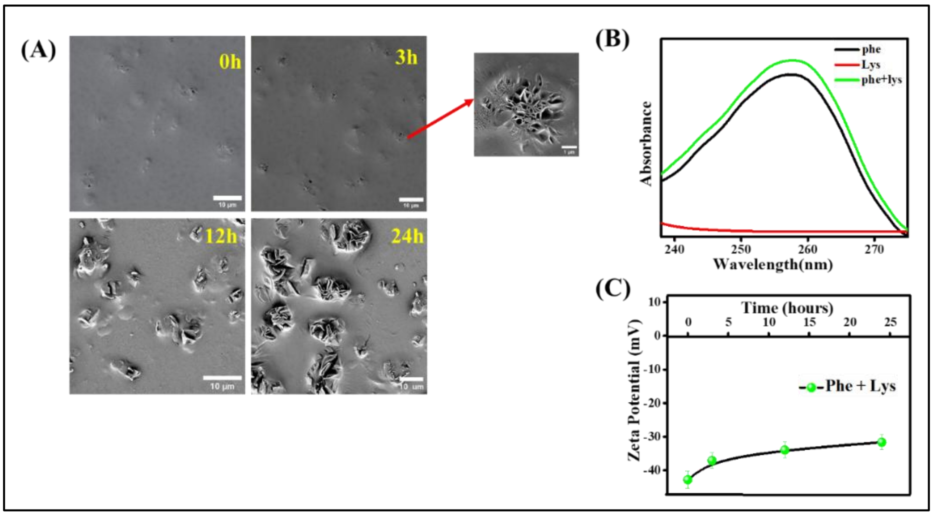

Figure 17: (A) Time-dependent SEM images of co-assembly of Phe and Lys (1:2 ratio), (B) UV-visible spectra of blank Phe, blank Lys, and co-assembly of Phe with Lys, (C) Time-dependent Zeta potential of co-assembly of Phe and Lys.

3.5 Co-assembly of phenylalanine and glutamic acid:

After that, we studied the interaction of Phe and Glu in a time-dependent manner. In OM images (Figure 18), we observed that blank Glu forms a small aggregate-like morphology at an initial stage and, for 24 hours, forms a leaf-like morphology. OM images (Figure 19) show that at a 1:1 ratio (phe: Glu), fibrillar morphology was present at the very initial stage, which confirms that Glu does not inhibit the fibrillar formation till 24 hours. In the case of a 1:2 ratio at an initial stage, fibrillar morphology was observed at the initial stage, but with time, we observed some aggregate formation starting, and at 3 hours, there was an aggregate with fibrillar morphology observed, and at 24 hours complete aggregate formed. For 1:3 at an initial stage, we observed fibrillar with aggregates, and at 3 hours observed large aggregates. For 1:4, a large aggregate morphology was observed. We further studied with a 1:2 ratio because in 1:2 we get a prominent intermediate. We confirmed this morphology for a 1:2 ratio with the CLSM microscopy. We used ThT, a well-known fluorescence marker for self-assembled fibrillar structures, and Nile red, a fluorescence marker for hydrophobic structures, to tag co-assembly (Figure 20). Also confirmed these results with SEM (Figure 21A).

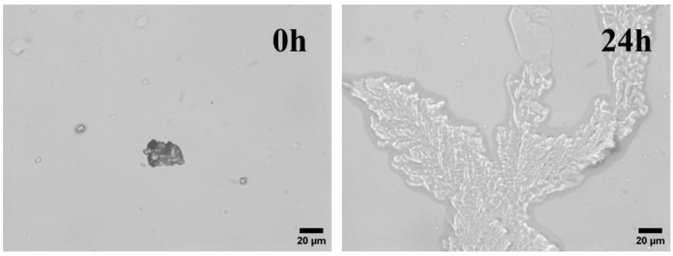

Figure 18: Time-dependent OM images of blank Glu. Scale bar – 20 µm.

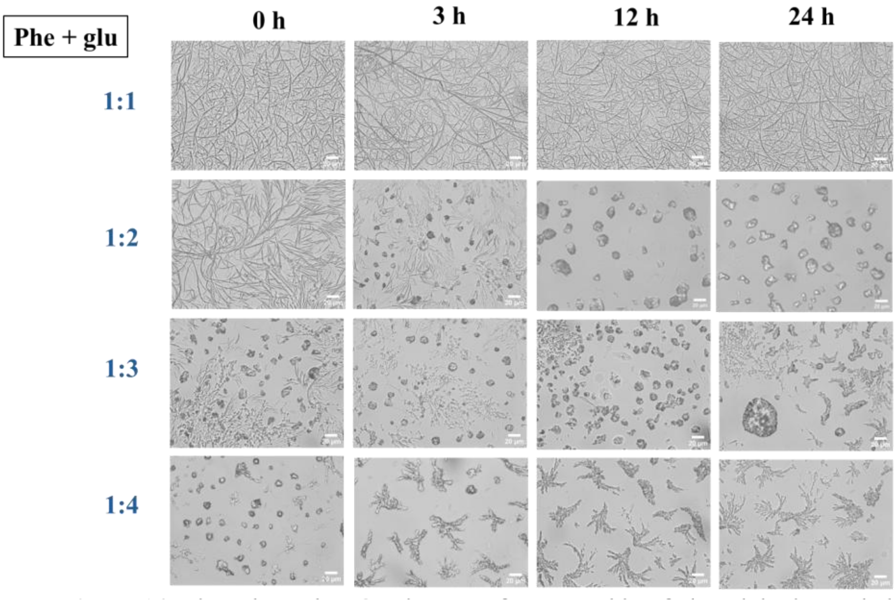

Figure 19: Time-dependent OM images of co-assembly of Phe and Glu. Scale bar – 20 µm.

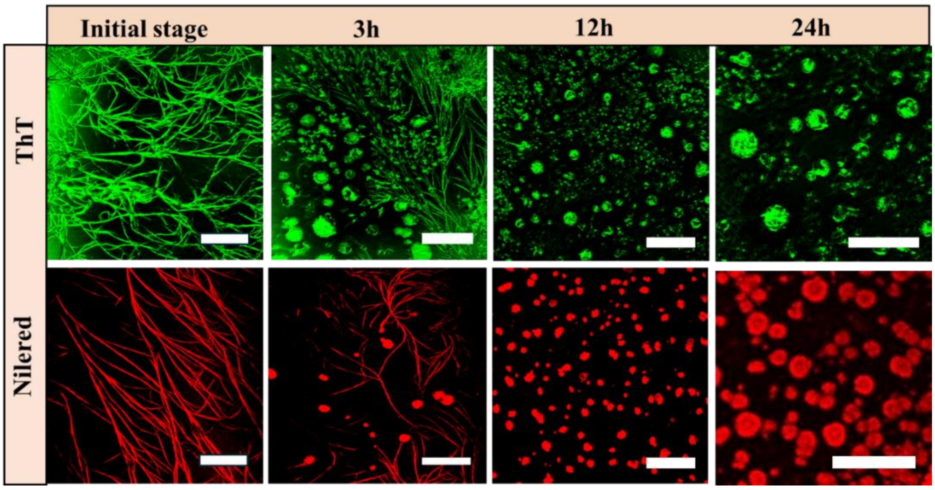

Figure 20: Time-dependent CLSM images of co-assembly of Phe and Glu (1:2 ratio). Scale bar - 10 µm.

To further study the effect of Glu interactions on the self-assembly of Phe, we performed UV-vis and Zeta potential. The UV-vis spectra (Figure 21B) of the co-assembly of Phe and Glu suggest an absorbance peak 258 nm of co-assembly intensity increased, which indicates the interactions between Phe and Glu. The shift happens may be due to the π−π stacking interactions between Phe and Glu. Zeta potential (Figure 21C) of co-assembly of Phe and Glu is negative, at the initial stage (-22.9), and with time zeta potential value changes and becomes less negative, and at 24 hours, we observed (-11.24). This may have happened due to structural changes.

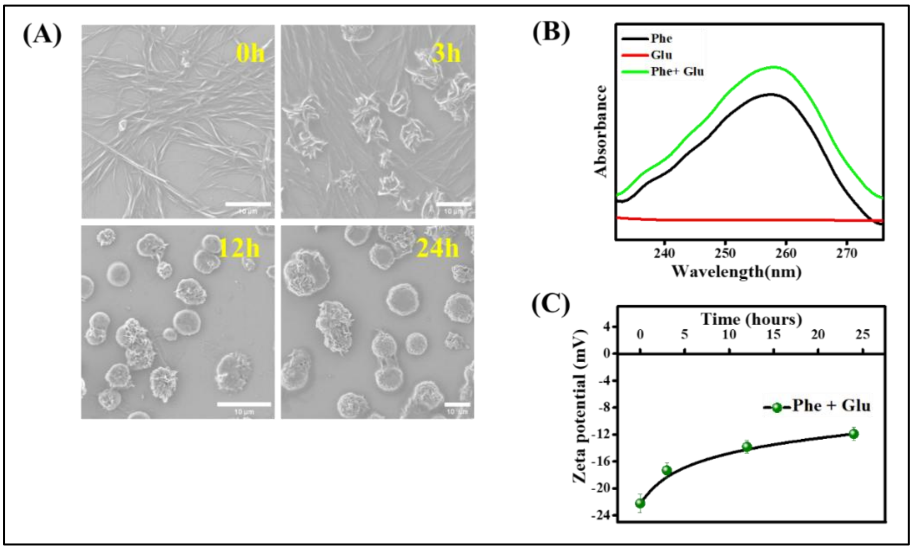

Figure 21:(A) Time-dependent SEM images of co-assembly of Phe and Glu (1:2 ratio), (B) UV-visible spectra of blank Phe, blank Glu, and co-assembly of Phe and Glu, (C) Time-dependent Zeta potential of co-assembly of Phe and Glu.

3.6 Co-assembly of phenylalanine and aspartic acid:

After that, we observed the interaction of Phe and Asp in a time-dependent manner. OM images (Figure 22) observed that blank aspartic acid at the initial stage, no prominent morphology is formed, but at 24 hours, a large leaf-like morphology is observed. OM images observed that at all ratios 1:1, 1:2, 1:3, and 1:4, fibrillar morphology was observed, which shows that aspartic acid does not affect the fibrillar formation process. (Figure 23) We also confirmed these results for a 1:2 ratio with CLSM images. We used ThT, a well-known fluorescence marker for self-assembled fibrillar structures, and Nile red, a fluorescence marker for hydrophobic structures, to tag co-assembly (Figure 24), We also confirmed the fibrillar morphology with SEM (Figure 25A).

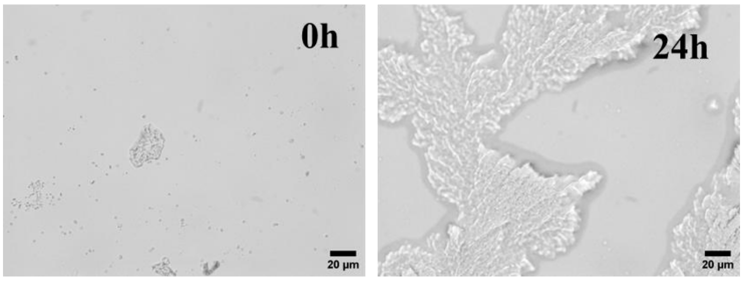

Figure 22: Time-dependent OM images of blank Asp. Scale bar – 20 µm.

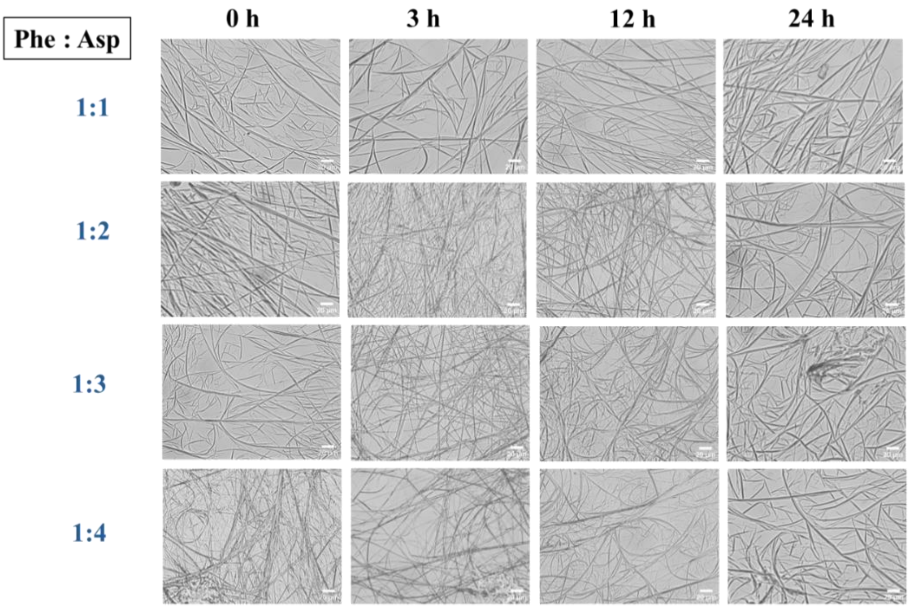

Figure 23: Time-dependent OM images of co-assembly of Phe and Asp. Scale bar – 20 μm.

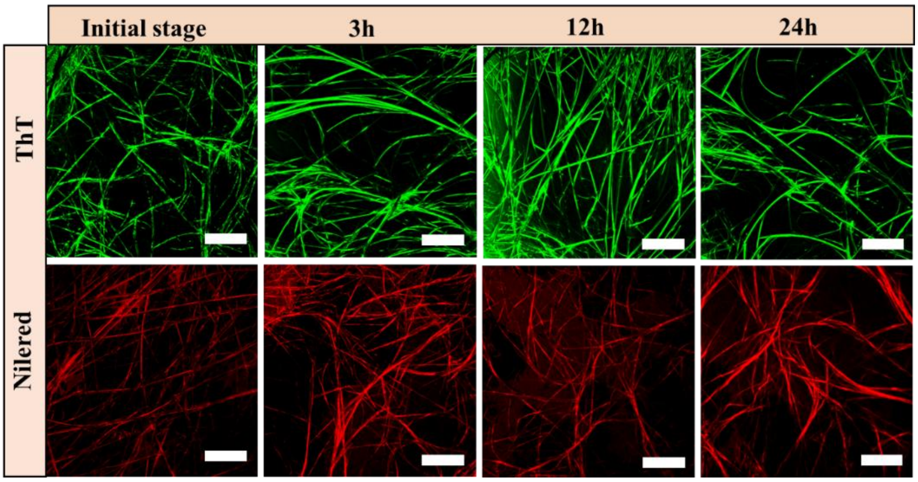

Figure 24: Time-dependent CLSM images of co-assembly of Phe and Asp (1:2 ratio). Scale bar – 20 μm.

To further study the effect of Asp interactions on the self-assembly of Phe, we performed UV-vis and Zeta potential. The UV-vis spectra (Figure 25B) of the co-assembly of Phe + Asp suggest that there are no changes compared to blank Phe, indicating that there is no structural changes occur. Zeta potential of co-assembly is observed negative, at the initial stage (-15.46) and remains negative till 24 hours, which indicates that the fibrillar structure stability. (Figure 25C)

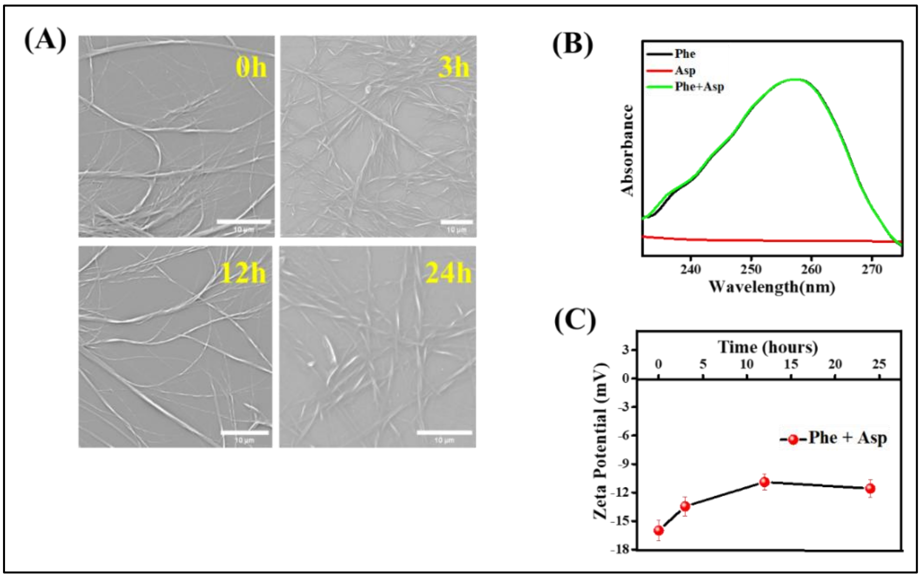

Figure 25: A) Time-dependent SEM images of co-assembly of Phe and Asp (1:2 ratio), (B) UV-visible spectra of blank Phe, blank Asp, and co-assembly of Phe and Asp, (C) Time-dependent Zeta potential of co-assembly of Phe and Asp.

3.7 Co-assembly of Phe-Phe and arginine:

In the case of Phe-amino acid co-assembly, the most significant morphological changes were observed at a 1:2 ratio of Phe to amino acids. Therefore, for Phe-Phe co-assembly, we consider only the 1:2 ratio of Phe-Phe to amino acids. In case of Phe-Phe and Arg co-assembly, time-dependent CLSM images (Figure 26) confirmed that at a 1:2 ratio, an aggregate-like morphology was observed at the initial stage to till 24 hours, and there is no fibrillar morphology was detected till 24 hours. These results are also confirmed with SEM images (Figure 27A). We further confirmed these results with UV-visible and Zeta potential. UV-visible spectra (Figure 27B) indicate that the intensity of the absorbance peak of the co-assembly of Phe-Phe and Arg increases compared to blank Phe, which suggests that there are structural changes occur, and this may be happened due to π-π interactions between Phe-Phe and Arg. Phe-Phe show negative zeta potential (-30.1) and Arg is positive charged amino acid and (Figure 27C) we get a negative zeta potential value for co-assembly, at the initial stage (-37.04), and along with time zeta potential value changed, and we observed (-29.21) after 24 hours. This observation indicates that the negative charge of the Phe-Phe self-assembly outer surface may interact with a positive charge of Arg, and these interactions could be a reason for the vesicle-like morphology formed in place of fibrillar morphology formation. And the zeta potential of co-assembly remains negative till 24 hours, which indicates structural stability.

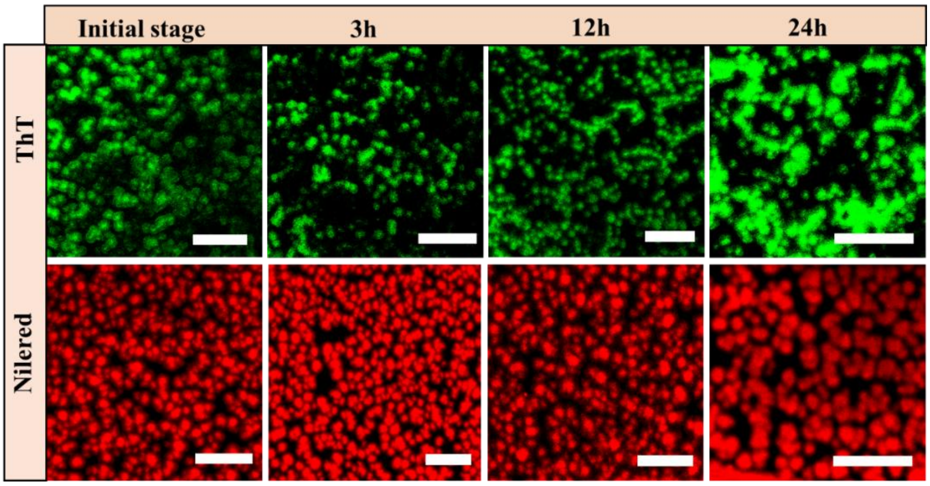

Figure 26: Time-dependent CLSM images of co-assembly of Phe-Phe and Arg (1:2 ratio). Scale bar - 10µm.

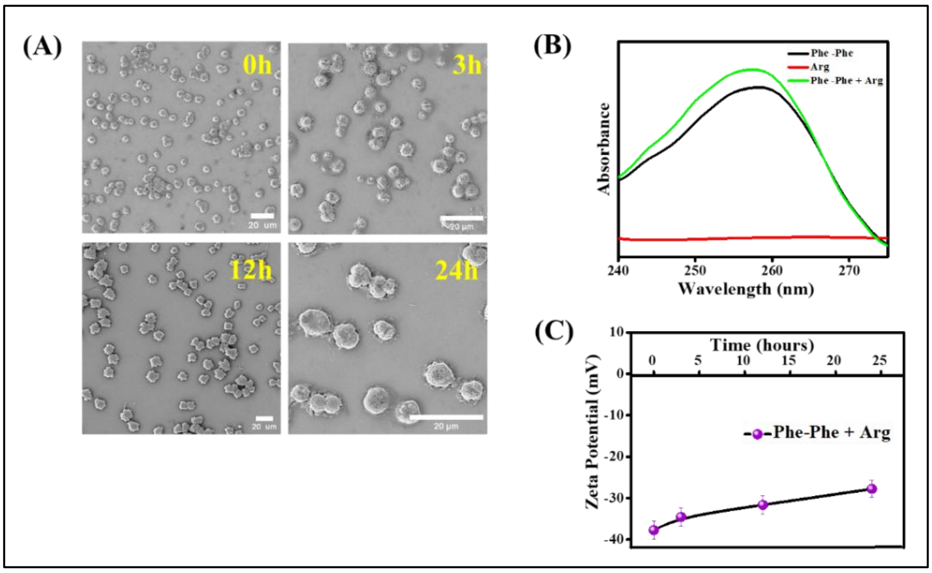

Figure 27: (A) Time-dependent SEM images of co-assembly of Phe-Phe and Arg (1:2 ratio), (B) UV-visible spectra of blank Phe, blank Arg, and co-assembly of Phe and Arg, (C) Time-dependent zeta potential of co-assembly of Phe-Phe and Arg.

3.8 Co-assembly of Phe-Phe and lysine:

Time-dependent CLSM images (Figure 28) confirmed that at a 1:2 ratio, an aggregate structure resembling a vesicle-like morphology was observed at the initial stage to till 24 hours, and there is no fibrillar morphology was detected till 24 hours. Also confirmed these results with SEM images (Figure 29A). we further confirmed these results with UV-visible and Zeta potential. UV-visible spectra (Figure 29B) indicate that the intensity of the absorbance peak of the co-assembly of Phe-Phe and Lys increases compared to blank Phe, which suggests that there are structural changes occur. Phe-Phe shows negative zeta potential (-30.1) and Lys is positive charged amino acid and (Figure 29C) we get a negative zeta potential value for co-assembly, at the initial stage (-40.1), and along with time zeta potential value changed, and we observed (-25.21) after 24 hours. This observation indicates that the negative charge of the Phe-Phe self-assembly outer surface may interact with a positive charge of Lys, and these interactions could be a reason for the vesicle-like morphology formed in place of fibrillar morphology formation. And the zeta potential of co-assembly remains negative till 24 hours, which indicates structural stability.

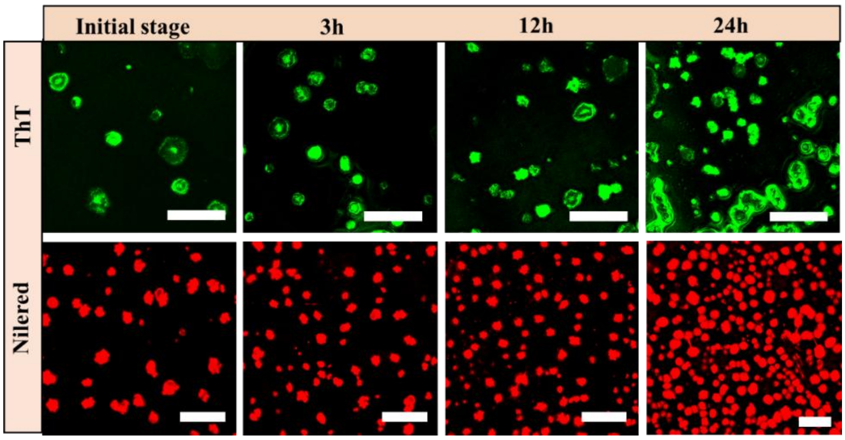

Figure 28: Time-dependent CLSM images of co-assembly of Phe-Phe and Lys (1:2 ratio). Scale bar - 20µm.

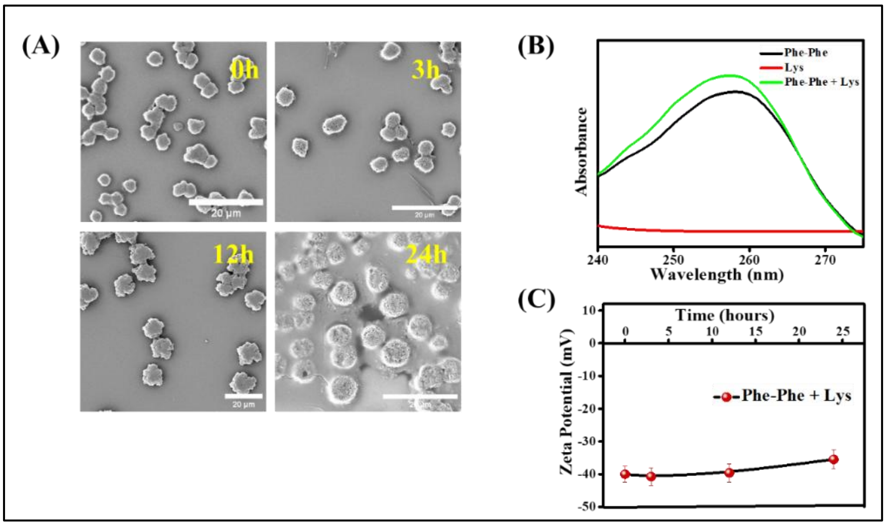

Figure 29: (A) Time-dependent SEM images of co-assembly of Phe-Phe and Lys (1:2 ratio), (B) UV-visible spectra of blank Phe-Phe, blank Lys, and co-assembly of Phe-Phe with Lys, (C) Time-dependent Zeta potential of co-assembly of Phe-Phe and Lys.

3.9 Co-assembly of Phe-Phe with glutamic acid and aspartic acid:

In the co-assembly of Phe-Phe with Glu and Phe-Phe with Asp, we observed fibrillar morphology with the naked eye (Figure 30A, B). (Figure 30C) shows the case of Phe-Phe self-assembly; no fibrillar morphology is observed with the naked eye. These indicate that Glu and

Asp promote the Phe-Phe fibrillar morphology formation. We confirmed these with CLSM images (Figure 31A) (Figure 32A), showing that there is fibrillar morphology in the initial stage to till 24 hours. Spectroscopic analysis was not performed further because the sample was turbid. However, zeta potential measurements indicate that there were no surface charge changes in the co-assembly's value over time for both the co-assembly. (Figure 31B) (Figure 32B)

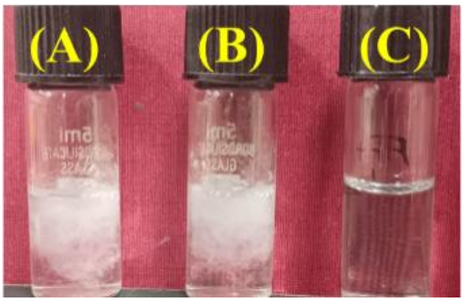

Figure 30: Images of (A) co-assembly of Phe-Phe and Glu, (B) co-assembly of Phe-Phe and Asp, (C) self-assembly of Phe-Phe.

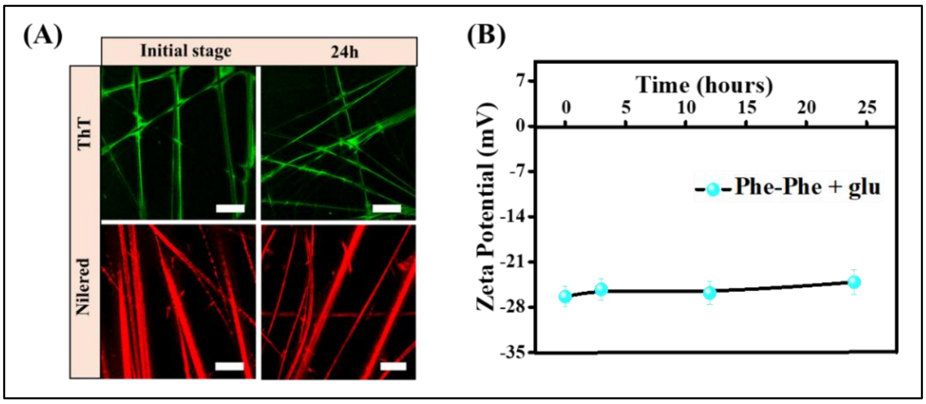

Figure 31: (A) Time-dependent CLSM images of co-assembly of Phe-Phe and Glu. Scale bar – 20 µm. (B) Time-dependent zeta potential of co-assembly of Phe-Phe and Glu.

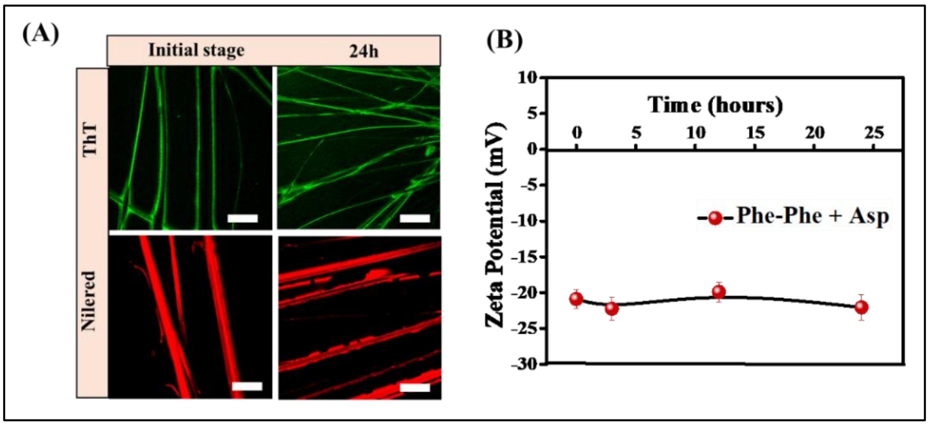

Figure 32: (A) Time-dependent CLSM images of Co-assembly of Phe-Phe and Asp. Scale bar – 20 µm. (B) Time-dependent zeta potential of co-assembly of Phe-Phe and Asp.

Future scope

In future research, we plan to conduct an in-depth investigation into the self-assembly mechanism of L-phenylalanine in the presence of polar amino acids. Specifically, we want to understand why these interesting structural changes happen during Phe-Glu co-assembly, even though both have negative surface charges. Our focus will be on elucidating the driving forces and structural transformations involved in the formation of various intermediates throughout the self-assembly process. Additionally, we are interested in exploring how these intermediates of Phe and Phe-Phe will interact with liposome vesicles.

Conclusions

In this study, we investigated the modulatory effects of various polar amino acids on the self-assembly of Phe and Phe-Phe. Our results demonstrate that the presence of different polar amino acids significantly alters the morphology. We draw the following conclusions from our observations.

a) We have observed that two basic amino acids, Arg and Lys, successfully inhibit the Phe and Phe-Phe fibrillar morphology.
b) We have observed that acidic amino acid Glu successfully inhibits the Phe fibrillation but promotes the Phe-Phe self-assembly process.
c) We have observed that acidic amino acid Asp doesn’t inhibit the Phe fibrillar morphology, but in the case of Phe-Phe promotes the self-assembly process.
d) We have successfully optimized the concentration ratio of Phe: polar amino acid (1:2), which shows prominent morphology and intermediates.

Supporting information

Here we show OM images of the co-assembly of Phe and polar amino acids (Ser, Thr, and Asn except Gln) which do not inhibit the fibrillar morphology of self-assembled Phe. We get fibrillar morphology till 24 hours.

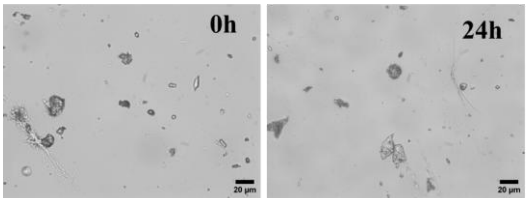

Figure S1: OM images of blank serine.

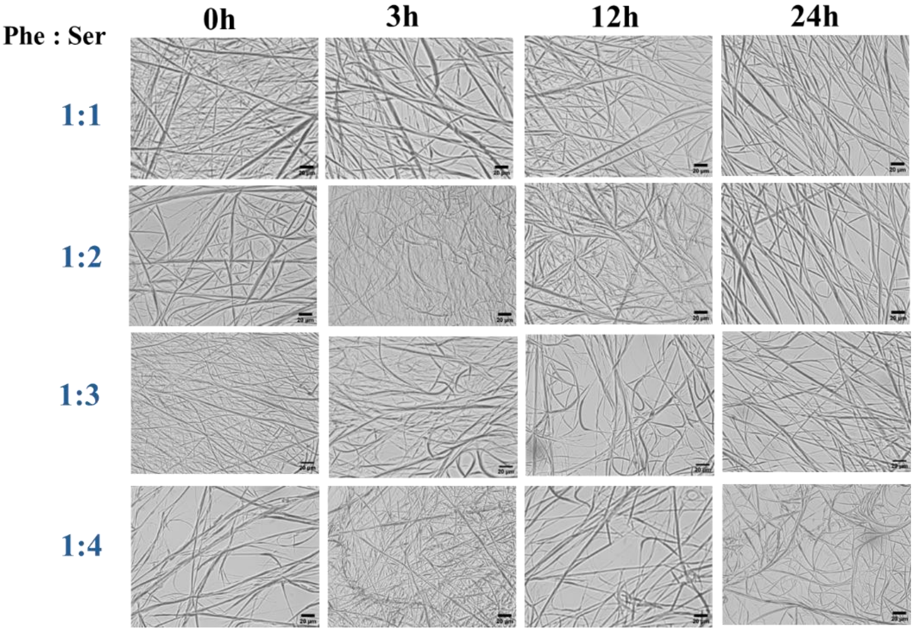

Figure S2: Time-dependent OM images of co-assembly of Phe and Ser.

OM images (Figure S1) show blank Ser self-assembly. OM images (Figure S2) show that at all concentrations, Ser does not inhibit the fibrillar morphology.

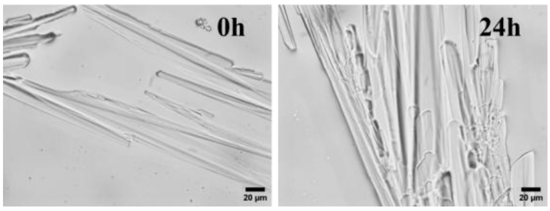

Figure S3: OM images of blank Thr.

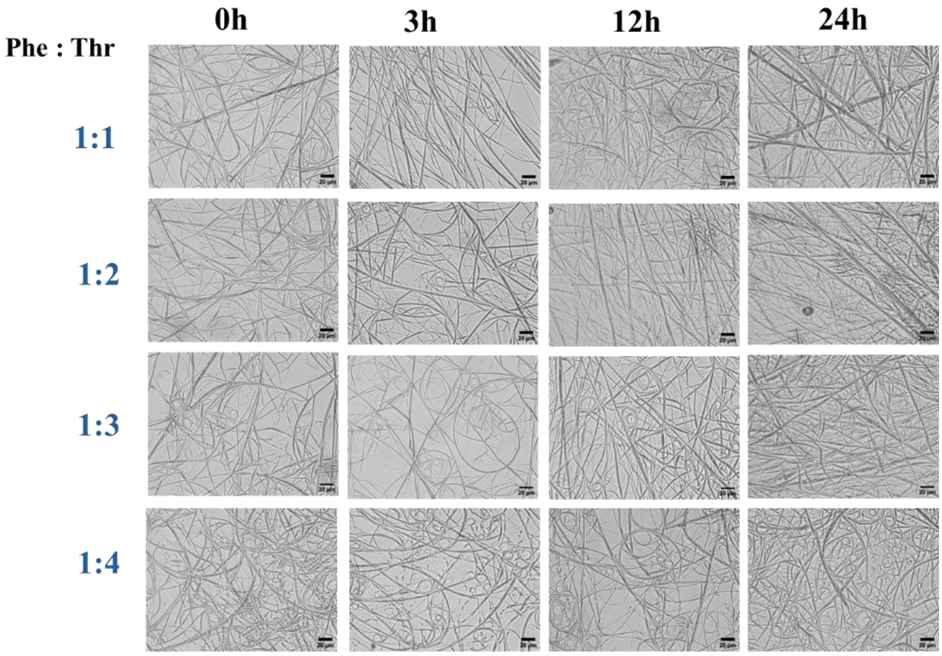

Figure S4: Time-dependent OM images of co-assembly of Phe and Thr.

OM images (Figure S3) show self-assembly of blank Thr. OM images (Figure S4) show that OM images show that there is fibrillar morphology, which means Thr does not show any effect on the Phe self-assembly process.

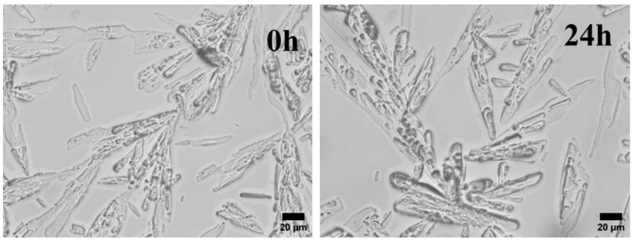

Figure S5: OM images of blank Glu.

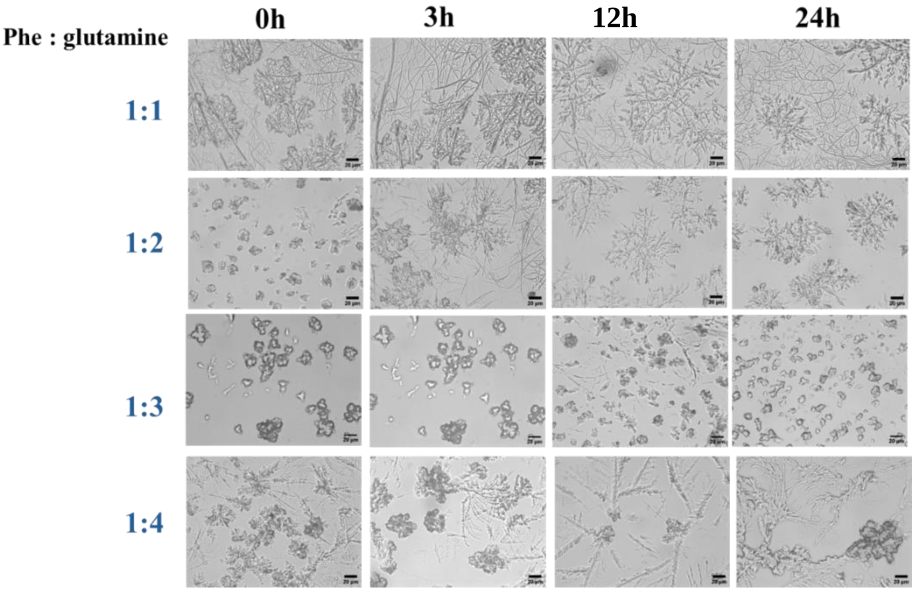

Figure S6: Time-dependent OM images of co-assembly of phenylalanine and Gln.

OM images (Figure S5) show self-assembly of blank Gln. OM images (Figure S6) show that Gln at a 1:1 ratio a little bit inhibits the fibrillar morphology and at a 1:2 ratio at the initial stage aggregate like morphology is observed and after that fibrillar aggregate morphology is formed till 24 hours and in 1:3 and 1:4 ratio aggregate formed, there is no any fibrillar morphology observed.

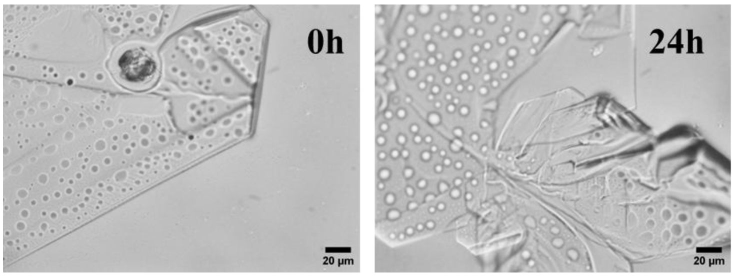

Figure S7: OM images of blank Asn.

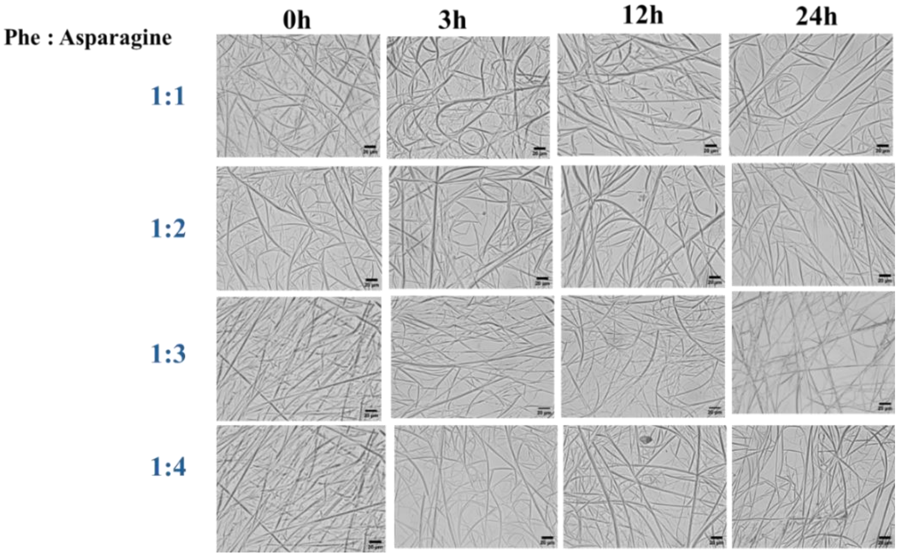

Figure S8: Time-dependent OM images of co-assembly Phe and Asn.

OM images (Figure S7) show self-assembly of blank Asn. OM images (Figure S8) show that in the co-assembly of Phe and Asn, there is fibrillar morphology observed.

References

1. Mandal, Dindyal, Amir Nasrolahi Shirazi, and Keykavous Parang. "Self-assembly of peptides to nanostructures." *Organic & biomolecular chemistry* 12, no. 22 **(2014)**: 3544-3561.

2. Northrop, Brian H., Yao-Rong Zheng, Ki-Whan Chi, and Peter J. Stang. "Self-organization in coordination-driven self-assembly." *Accounts of chemical research* 42, no. 10 **(2009)**: 1554-1563.

3. Yang, Bin, Dave J. Adams, Maria Marlow, and Mischa Zelzer. "Surface-mediated supramolecular self-assembly of protein, peptide, and nucleoside derivatives: from surface design to the underlying mechanism and tailored functions." *Langmuir* 34, no. 50 **(2018)**: 15109-15125.

4. Cosert, K. M., Angelines Castro-Forero, Rebecca J. Steidl, Robert M. Worden, and G. Reguera. "Bottom-up fabrication of protein nanowires via controlled self-assembly of recombinant Geobacter pilins." *MBio* 10, no. 6 **(2019)**: 10-1128.

5. Abbas, Manzar, Qianli Zou, Shukun Li, and Xuehai Yan. "Self-assembled peptide-and protein-based nanomaterials for antitumor photodynamic and photothermal therapy." *Advanced materials* 29, no. 12 **(2017)**: 1605021.

6. Knowles, Tuomas PJ, Michele Vendruscolo, and Christopher M. Dobson. "The amyloid state and its association with protein misfolding diseases." *Nature reviews Molecular cell biology* 15, no. 6 **(2014)**: 384-396.

7. Aguzzi, Adriano, and Tracy O'connor. "Protein aggregation diseases: pathogenicity and therapeutic perspectives." *Nature reviews Drug discovery* 9, no. 3 **(2010)**: 237-248.

8. Zaguri, D.; Kreiser, T.; Shaham-Niv, S.; Gazit, E. Antibodies towards tyrosine amyloid like fibrils allow toxicity modulation and cellular imaging of the assemblies. *Molecules* **2018**, 23, 1273.

9. Adler-Abramovich, L.; Vaks, L.; Carny, O.; Trudler, D.; Magno, A.; Caflisch, A.; Frenkel, D.; Gazit, *E. Nat. Chem. Biol*. **2012**, 8, 701–706. doi:10.1038/nchembio.1002

10. Banik, D.; Kundu, S.; Banerjee, P.; Dutta, R.; Sarkar, N. Investigation of fibril forming mechanisms of L-phenylalanine and L-tyrosine: Microscopic insight toward phenylketonuria and tyrosinemia type II. J. *Phys. Chem*. B **2017**, 121, 1533−1543.

11. Li, R.; Wu, Z.; Wangb, Y.; Ding, L.; Wang, Y. Role of pH induced structural change in protein aggregation in foam fractionation of bovine serum albumin. *Biotechnol. Rep*. **2016**, 9, 46−52.

12. Klement, K.; Wieligmann, K.; Meinhardt, J.; Hortschansky, P.; Richter, W.; Fandrich, M. Effect of different salt ions on the propensity of aggregation and on the structure of Alzheimer's Aβ(1−40) amyloid fibrils. *J. Mol. Biol.* **2007**, 373, 1321−1333.

13. Banik, Debasis, Rupam Dutta, Pavel Banerjee, Sangita Kundu, and Nilmoni Sarkar. "Inhibition of fibrillar assemblies of l-phenylalanine by crown ethers: a potential approach toward phenylketonuria." *The Journal of Physical Chemistry B* 120, no. 31 **(2016)**: 7662-7670.

14. Shaham-Niv, Shira, Pavel Rehak, Dor Zaguri, Aviad Levin, Lihi Adler-Abramovich, Lela Vuković, Petr Král, and Ehud Gazit. "Differential inhibition of metabolite amyloid formation by generic fibrillation-modifying polyphenols." *Communications Chemistry* 1, no. 1 **(2018)**: 25.

15. Kour, Avneet, Taru Dube, Ashwani Kumar, and Jiban Jyoti Panda. "Anti-Amyloidogenic and Fibril-Disaggregating Potency of the Levodopa-Functionalized Gold Nanoroses as Exemplified in a Diphenylalanine-Based Amyloid Model." *Bioconjugate Chemistry* 33, no. 2 **(2022)**: 397-410.

16. Singh, Virender, Ratan Kumar Rai, Ashish Arora, Neeraj Sinha, and Ashwani Kumar Thakur. "Therapeutic implication of L-phenylalanine aggregation mechanism and its modulation by D-phenylalanine in phenylketonuria." *Scientific reports* 4, no. 1 **(2014)**: 3875.

17. Singh, Prabhjot, Satish K. Pandey, Aarzoo Grover, Rohit K. Sharma, and Nishima Wangoo. "Understanding the self-ordering of amino acids into supramolecular architectures: co-assembly-based

modulation of phenylalanine nanofibrils." *Materials Chemistry Frontiers* 5, no. 4 **(2021)**: 1971-1981.

18. Bagchi, D.; Maity, A.; De, S. K.; Chakraborty, A. Effect of Metal Ions on the Intrinsic Blue Fluorescence Property and Morphology of Aromatic Amino Acid Self-Assembly. *J. Phys. Chem*. B **2021**, 125,12436−12445.

19. Mandal, Dindyal, Amir Nasrolahi Shirazi, and Keykavous Parang. "Self-assembly of peptides to nanostructures." *Organic & biomolecular chemistry* 12, no. 22 **(2014)**: 3544-3561.

20. Northrop, Brian H., Yao-Rong Zheng, Ki-Whan Chi, and Peter J. Stang. "Self-organization in coordination-driven self-assembly." *Accounts of chemical research* 42, no. 10 **(2009)**: 1554-1563.

21. Knowles, T. P. J., Vendruscolo, M., & Dobson, C. M. **(2014)**. The amyloid state and its association with protein misfolding diseases. *Nature Reviews Molecular Cell Biology*, 15(6), 384–396.

22. Hartgerink, J. D., Beniash, E., & Stupp, S. I. **(2001)**. Self-assembly and mineralization of peptide-amphiphile nanofibers. *Science*, 294(5547), 1684–1688.

23. Görbitz, C. H. The Structure of Nanotubes Formed by Diphenylalanine, the Core Recognition Motif of Alzheimer’s β-Amyloid Polypeptide. *Chem. Commun.* **2006**, No. 22, 2332–2334.

24. Noy, D.; Solomonov, I.; Sinkevich, O.; Arad, T.; Kjaer, K.; Sagi, I. Zinc-amyloid β interactions on a millisecond timescale stabilize non-fibrillar Alzheimer-related species. J. Am. Chem. Soc. **2008**, 130, 1376−1383.

25. Tomar, Deepak, Shilpi Chaudhary, and Kailash Chandra Jena. "Self-assembly of L-phenylalanine amino acid: electrostatic induced hindrance of fibril formation." *RSC advances* 9.22 **(2019)**: 12596-12605.

26. Klement, K.; Wieligmann, K.; Meinhardt, J.; Hortschansky, P.; Richter, W.; Fandrich, M. Effect of different salt ions on the propensity of aggregation and on the structure of Alzheimer's Aβ amyloid fibrils. J. Mol. Biol. **2007**, 373, 1321−1333.

27. Li, R.; Wu, Z.; Wangb, Y.; Ding, L.; Wang, Y. Role of pH induced structural change in protein aggregation in foam fractionation of bovine serum albumin. *Biotechnol. Rep*. **2016**, 9,46−52.

28. Yumoto, S.; Kakimi, S.; Ohsaki, A.; Ishikawa, A. Demonstration of aluminium in amyloid fibers in the cores of senile plaques in the brains of patients with Alzheimer's disease. *J. Inorg. Biochem*. **2009**, 103, 1579−1584.

29. Ha, C.; Ryu, J.; Park, C. B. Metal ions differentially influence the aggregation and deposition of Alzheimer's β-amyloid on a solid template. *Biochemistry* **2007**, 46, 6118−6125.

30. Ye, X.; Capezza, A.; Xiao, X.; Lendel, C.; Hedenqvist, M.; Kessler, V.; Olsson, R. Protein nanofibrils and their hydrogel formation with metal ions. *ACS Nano* **2021**, 15 (3), 5341−5354.

31. Debanjan Bagchi, Avijit Maity, Anjan Chakraborty. Metal Ion-Induced Unusual Stability of the Metastable Vesicle-like Intermediates Evolving during the Self-Assembly of Phenylalanine: Prominent Role of Surface Charge Inversion. *The Journal of Physical Chemistry Letters* **2024**, *15* (16) , 4468-4476.